2009-01-01

Hybrid Ftth Optical Network Using Incoherent Optical Code Division Multiple Access

Joel Quintana
University of Texas at El Paso, joel.jquintana@gmail.com

HYBRID FTTH OPTICAL NETWORK USING INCOHERENT OPTICAL CODE DIVISION MULTIPLE ACCESS

JOEL QUINTANA

Department of Electrical and Computer Engineering

APPROVED:

_____
Virgilio Gonzalez, Ph.D., Chair

_____
Jose G. Rosiles, Ph.D.

_____
Rolfe Sassenfeld, Ph.D.

_____
Patricia D. Witherspoon, Ph.D.
Dean of the Graduate School

To my parents, Rosalia & Rafael,

my bother Juan Rene, my nephews Fabian & Sophia,

and my fiancé Marcy.

HYBRID OPTICAL NETWORK USING INCOHERENT OPTICAL CODE DIVISION MULTIPLE ACCESS VIA OPTICAL DELAY LINES

by

JOEL QUINTANA, B.S.E.E.

THESIS

Presented to the Faculty of the Graduate School of

The University of Texas at El Paso

in Partial Fulfillment

of the Requirements

for the Degree of

MASTER OF SCIENCE

Department of Electrical & Computer Engineering

THE UNIVERSITY OF TEXAS AT EL PASO

May 2009

ACKNOWLEDGEMENTS

First of all I want to thank my parents, they're guidance and unconditional love have been the fuel to my achievements. My mother Rosalia, who made me the man that I am today, whose wisdom and teaching far transcends any college education. The lifelong dedication and sacrifice to her sons is an astonishing, and I feel blessed beyond comprehension to have a mother like her. My father Raphael, the smartest man I have ever known. Because of him, I have a thirst for knowledge that drove me to begin this thesis. My brother Rene, whose incredible discipline, intelligence, and support helped me make the right decisions in life, without his guidance I would not be writing these acknowledgements.

My appreciation to all at the UTEP Electrical and Computer Engineering Department is immeasurable. My advisor Dr. Virgilio Gonzalez, whose only concern was my education and growth; whose only question was "what do you need?" and was an inspiration for continuing education and the desire to educate others. All the professors that answered questions about course work, engineering, or otherwise, thank you for your collective knowledge and wisdom; whether it be on fundamentals of electromagnetism and Fourier transforms, or the current state of property taxes in the state of California. The staff: Suki Quezada and Ralph Loya undoubtedly the mother and father figure for all the students in the department. Thanks to Gabby Gandara for all his help and guidance in becoming a successful student and above all a professional.

To all my friends and relatives, who showed me how to have fun and not take myself too seriously, or anyone else for that matter. All my best memories include them. My fiancé Marcy

whose love and support make me feel as there's no problem I can't solve. I feel honored that you will have me be your husband. Thank you all!!

ABSTRACT

Over the past 20 years there has been extensive research on the application of spread spectrum multiplexing techniques for communications via optical fiber. Optical Code Division Multiplexing (OCDMA) is the technique that has exhibited the most promise as a primary multiplexing vehicle for the transition into all-optical processing of data, and as a supplement to other techniques such as Time Division Multiplexing (TDM) and Wave Division Multiplexing (WDM). OCDMA can be classified into *incoherent* OCDMA, where coding and detection is done on the basis of optical power, and *coherent* OCDMA where coding is done on a field amplitude basis. The commercialization of these technologies has been a slow process as interferometic noise (know as beat noise), multiuser access interference (MAI) and optical component cost are the major hurdles.

This thesis concentrates on the application of incoherent OCDMA on a Fiber to the Home (FTTH) type access network where users receive information from a central terminal that is OCDMA encoded electronically. Only the user with the proper optical decoding stage will be able to discriminate and reconstruct the original information. The decoding is done via passive optical delay lines performing a convolution between the electrical *orthogonal optical code* (OOC) and the impulse response of the optical delay lines. The result is an autocorrelation peak or a crosscorrelation that provides no outstanding optical intensity peak.

This document analyzes the proper autocorrelation and crosscorrelation waveforms for 2 users on this "hybrid" OCDMA coding scheme and defines threshold, beat noise mitigation and information reconstruction techniques for further expansion of the network.

TABLE OF CONTENTS

LIST OF TABLES

LIST OF FIGURES

1 INTRODUCTION

Communications networks are directly linked to our economy, national security, and our way of life. With such a huge demand and need for worldwide information; fiber optics and its ultra high data capacity becomes a very attractive, and to a certain extent, necessary solution. Today's deployment of optical networks serve the purpose of point-to-point data transmission carrying data from several sources through optical signals multiplexed in a single fiber. These signals are transmitted through the fiber at aggregated data-rates well over the Terabits per second range. Most data processing such as routing, repeating, and amplification are still performed with electronic data links. This periodic conversion from optical to electrical causes data-rate "bottlenecks" at these processing nodes at approximately 40 Gigabits per second.

It is well known that the most critical segment of any network is the last mile, also known as the access network, because it provides the information link to businesses and consumers who provide revenues. Spread spectrum multiplexing techniques in the form of Code Division Multiple Access, have been investigated extensively for mobile and satellite communications and offer promising solutions for optical access networks as it offers the following advantages: All optical processing, fully asynchronous transmission, low-delay access, soft capacity on demand, potential security, and quality of service control [1] [2] [3]. This thesis concentrates on the implementation of a Fiber to the Home (FTTH) access network topology using temporal incoherent OCDMA. The encoding takes place at a distribution center in electrical while the decoding is done at each user with optical delay lines.

1.1 Structure of Thesis

To understand the research presented in this document, I strongly believe that a brief summary of fiber optic fundamentals is necessary. Chapter 1 presents these fundamentals in the following manner: optical fiber communication basics, light wave transmission properties, and fiber optic communication principles. Chapter 2 defines the scope of research and a discussion of the literature reviewed to establish the work presented in this thesis. Broad investigations in OCDMA have addressed the possibilities of implementing CDMA in the optics domain. The experiment methodology is explained in Chapter 3, Elaborating on network configuration, the coding scheme, and the analysis criteria; where upon the results will be referenced. Chapter 4 describes the experiment results and Chapter 5 will conclude the paper with future works and experimental conclusions.

1.2 What is Optical Fiber?

An optical fiber is a thin (on the order of 2 to 125 μm), flexible, medium that's capable of guiding light. Optical fibers are made from various glass and plastics. It has been found however that ultrapure fused silica exhibits the lowest losses of light. Ultrapure silica is extremely difficult and expensive to manufacture; multi-component glass fibers with higher losses are more economical and provide good performance. Plastic fiber is the least costly of the optical fiber materials; it experiences high optical transmission loss which is acceptable for short haul and audio applications [4]. An optical fiber has a cylindrical shape and consists of three concentric sections: the core, the cladding and the jacket. The core is glass or plastic and is typically 8 to 50 μm. The core is surround by the cladding, also made of glass or plastic and is

typically 125 μm in diameter.

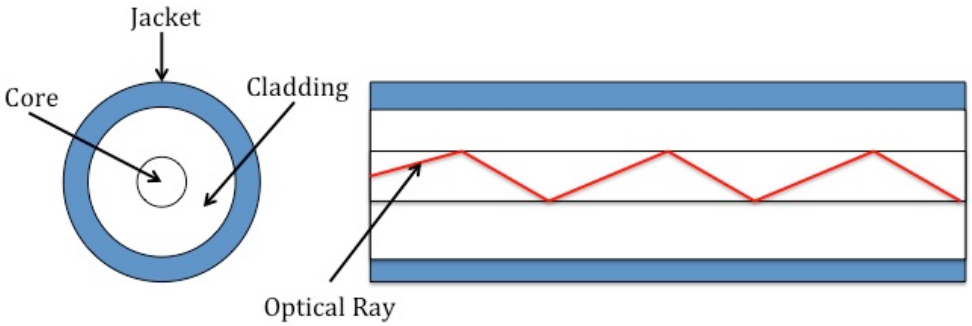

Figure 1: Optical Fiber

The core and the cladding have different optical properties, mainly the index of refraction (which will be explain later in more detail). The difference in index of refraction at the interface between the core and the cladding trap light rays traveling though the core by a phenomenon known as *total internal reflection*. The outer layer known as the jacket, is a plastic or other material layered to protect against moisture, crushing, abrasion, and other environmental damages [4]. A simple example of the propagation of light in an optical fiber and its different components are depicted in figure 1.

1.2.1 Basic Optical Communications Model

In order to transmit information through optical fibers, the following fundamental components are needed: a data source, a light source, optical fiber, a light detector, and a data receiver. Figure 2 shows an example of how a telephone conversation is transmitted through fiber a fiber optic link. The voice of the user is introduced into the system by the handset's microphone, and then translated into a series of bits. The bits representing the voice modulate the optical transmitter, which consists of a semiconductor laser or light-emitting diode (LED). Light bearing the information travels through the optical fiber to the detector on the other end.

The light source usually radiates in the near-infrared portion of the electromagnetic spectrum where the transmission characteristics of optical fibers are best utilized [5].

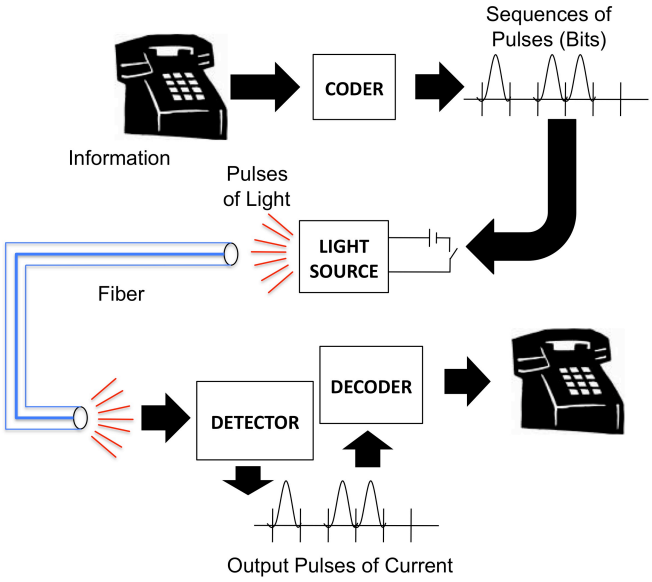

Figure 2: Basic Optical System, Telephone Call Example

Once at the detector, a photodiode produces a current proportional to the intensity of the light bearing the information. In other words, converting the signal from optical to electrical. Once in the electrical domain the bits are decoded and the audio signal can be heard on the receiving phone. The fundamental components in the preceding example are in all optical communication systems.

1.2.2 Electromagnetic Wave Properties of Light

The nature of light is characterized by the "wave-particle duality" principle. The propagation of light is governed by its particle properties, whereas the exchange of energy between light with matter is governed by its particle properties [6]. A particle of light has energy *E* given by:

$$E = hf = \frac{hc}{\lambda} \qquad (1)$$

where f is frequency, l is wavelength, c is the speed of light, and h is Plank's Constant

$$h = 6.626 \times 10^{-34}\ J \cdot s = 4.136 \times 10^{-15}\ eV \cdot s. \qquad (2)$$

Optical communications use frequencies in a specific region of the spectrum, mainly in the visual and infrared ranges, hence the word "optics". Light moves through fiber optic like an electromagnetic wave through a waveguide, however to more easily represent this propagation; ray theory is often used.

1.2.2.1 EM Spectrum in Optical Communications

The visual region of the spectrum is approximately 400 to 700 nm. These limits correspond to the color blue and red and bordered by the ultraviolet and infrared regions respectively.

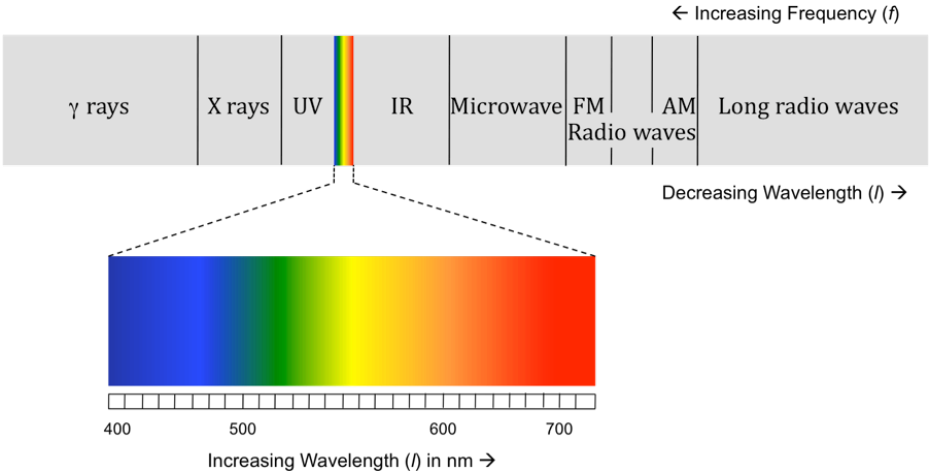

Figure 3: EM Spectrum

In telecommunications with optical waveguides the near-infrared wavelength range of 800-1600nm is used, with the preferred wavelengths being 850, 1310, and 1550 nm [7]. These wavelengths exhibit the least amount of attenuation when propagating through the fiber optic

material. There are some systems that do use the 680 nm wavelength, these are usually high end audio systems with links less than 10 m in length.

1.2.2.2 Wave Equation

In general, a wave is understood to be the propagation of a condition or its generation in a medium without actually transporting the mass or material of the medium itself [7]. A light wave's condition is that of an electromagnetic field propagating through a transparent medium, or in this case, silica or plastic fiber optics. In the simplest case, an electromagnetic wave can be described as a sine function. As the wave propagates through the fiber, its general displacement a in the z direction can be described in the following manner:

$$a = A\sin(\omega t - kz) = A\sin 2\pi\left(\frac{t}{T} - \frac{z}{\lambda}\right), \qquad (3)$$

a	displacement of a plane wave
A	amplitude in units of the displacement
w	angular frequency in s^{-1}
t	time in s
k	wave number in m^{-1}
z	length in z direction in m
T	period of oscillation in s
l	wavelength in m

For the rest of this document, we can consider the direction z being the direction associated with the length of the fiber.

1.2.2.3 Ray Theory

An alternative method to analyzing optical waveguides is through the use of a geometric or ray optics model. Using ray optics allows a simplified approach to describing how light-waves travel in the optical fiber and how different scenarios affect the geometric behavior of light-waves in the fiber.

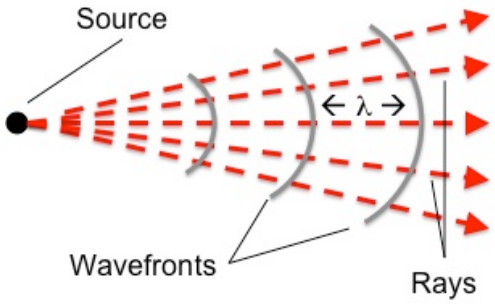

Figure 4: Ray Theory

Ray optics is very similar to the classical mechanics of a point particle [5], The motion of wave fronts can be represented by rays drawn perpendicular to the wave fronts. For a point source, the rays are radial lines diverging from the source [6]. A pictorial representation is depicted in figure 4.

1.2.3 Light-Ray Propagation in Optical Fibers

Light traveling in an optical fiber is simply an electromagnetic wave front propagating in a dielectric waveguide. In a vacuum, light rays travel at a velocity of $3\times10^{8} m/s$. In any other medium light rays travel slower given by

$$v = \frac{c}{n} \qquad (4)$$

where n is the index of refraction of the material. Note the speed of light in a vacuum is 1. Air and gasses have a refractive index $n \approx 1$. The index for water is approximately 1.33 for optical frequencies. Glass, which is primarily used in optical fiber, is comprised of many compositions and therefore each has its unique refractive index. Most silica fibers have an approximate index of 1.5 more precisely the values lie between 1.45 and 1.48. Below is a table of refractive indices' for some common materials.

Table 1: Index of refraction for some materials

Material	Index of Refraction
Air	1.00
Carbon Dioxide	1.00
Water	1.33
Silica glass	1.50
Sodium Chloride	1.54
Sapphire	1.80

1.2.3.1 Total Internal Reflection

When a light ray crosses a change of medium, ray theory states that, at a plane boundary, a ray is reflected at an angle equal to the angle of incidence θ_i with respect to the interface normal.

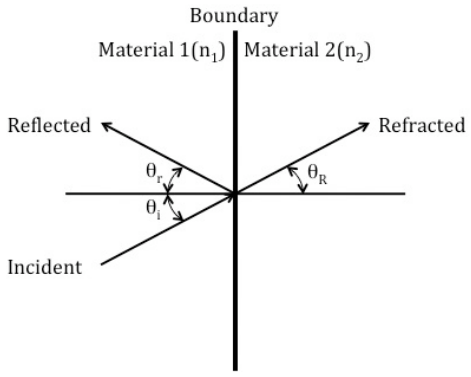

Figure 5: Incident, transmitted, & reflected ray at a boundary between two materials

Referring to figure 5, it is clear that $\theta_i = \theta_r$, where θ_r is the angle of reflection. The angle at which the refracted ray enters the new material is then given by Snell's law

$$\frac{\sin\theta_R}{\sin\theta_i} = \frac{n_1}{n_2}. \qquad (5)$$

The angle of refraction θ_R is less than the angle of incidence if $n_1 < n_2$. In other words, the refracted ray is bent towards the normal when the ray is traveling from a material having a lower refractive index. The opposite is true for a ray traveling from a material with index of

refraction n_1 greater than the index of refraction n_2 of the new medium. In which the angle of the refracted ray is bent away from the normal.

Snell's law indicates that refraction cannot take place when the angle of incidence is too large [8]. Light cannot escape the material boundary if the angle of incidence makes the sine of the angle of refraction θ_R equal to 1.0. This makes the angle of the refracted ray 90^o, where the light travels along the boundary. This incidence angle is called *the critical angle*.

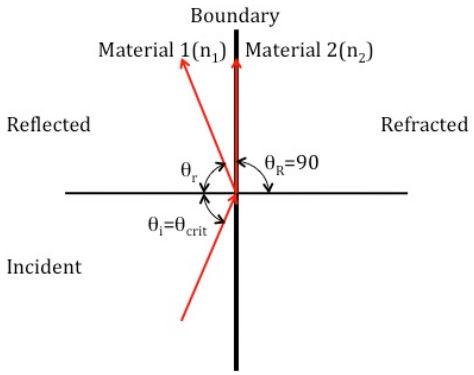

Figure 6: Incident Ray at Critical Angle resulting in Total Internal Reflection

The concept of critical angle is particularly important because this is how we explain the guiding of light through transparent optical fibers. This phenomenon of trapping a light ray within a material is known as *total internal reflection*. The critical angle if easily derived from Snell's law to give

$$\theta_{crit} = \arcsin(\frac{n_2}{n_1}). \qquad (6)$$

1.2.3.2 Attenuation and Dispersion

As light travels in the fiber core it undergoes various losses. These losses can be categorized into two groups; absorption and scattering. The total attenuation of light intensity is the sum of all the phenomena previously listed. Attenuation limits how far a light signal

representing information can travel before said information is lost. Absorption of light depends greatly on the wavelength and the material it passes through. Absorption is uniform and cumulative through the material. The same amount of the same material always absorbs the same fraction of light.

Atoms and other particles inevitably scatter some of the light that hits them. The light isn't absorbed, just sent in a different direction[8]. This process is called *Rayleigh scattering*. Scattering not only depends on the specific type of material but on the size of scattering particles found in the material. If the particle size is comparable to the wavelength the more scattering with occur. Scattering like absorption is also uniform and cumulative through the fiber material. Both scattering and absorption contribute to the total attenuation found in fiber, however, when transmitting light through a fiber the distinction between absorption and scattering is of no importance. Fiber links are limited in path length by attenuation and by pulse distortion (or dispersion)[9]. Dispersion is the spreading of a light pulse as it travels along the fiber. For Example; Light representing a single pulse traveling through the optical fiber takes different paths, along the waveguide.

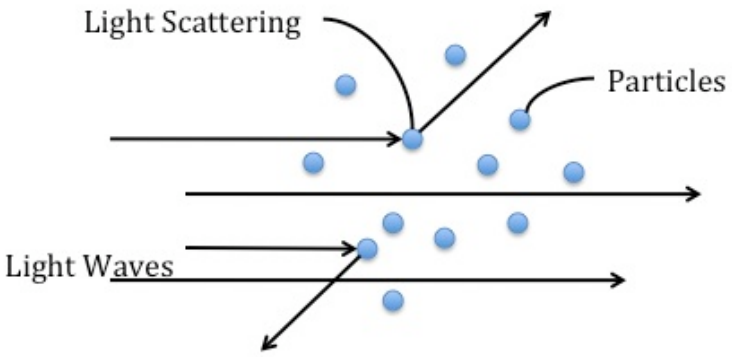

Figure 7: Rayleigh scattering

The different rays reach the end of the fiber at different times. This time depends on the overall distance a particular ray travels to reach the end. This is more apparent in multimode

fiber, whose core diameter is much bigger than the wavelength of light and allows many wave modes to propagate. To mitigate this problem single mode fiber was developed. This fiber has a core diameter of approximately 9 mm (compared to 62.5 mm of multi-mode) and allows only one mode to propagate.

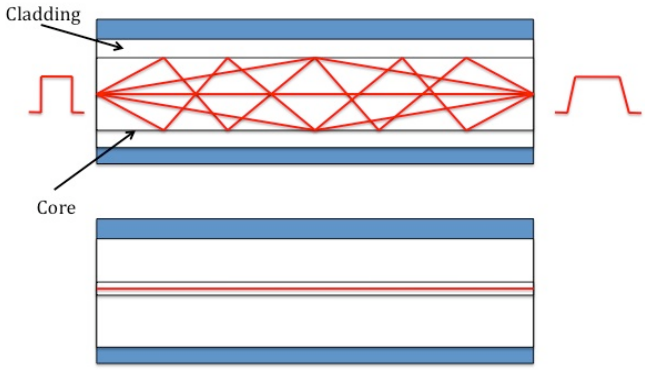

Figure 8: Dispersion in MM (top) vs. SM (bottom)

Today single mode fiber is used extensively in high speed and long distance optical communications due to its ability to sustain pulse with for 100km without major dispersion effects. For this thesis experiment only single mode optical fiber is used.

1.3 Fiber Optic Communications

Optical fibers are widely deployed today in all kinds of telecommunications networks, except perhaps in residential access areas[10]. Networks that use optical fibers offer a common infrastructure over which a variety of services can be delivered. Optical fibers offer a much higher bandwidth and are less susceptible to electromagnetic interference over copper cables. For this reason, fiber optics is the preferred medium for high-speed (>10Mbps) communications for distances over 1 kilometer, and for short-run (<500m) distances with data rates greater than gigabits for second.

1.3.1 Bandwidth

Transmission *capacity* or *bandwidth* tells us how much information a system can carry. The more information you want to transmit the faster the signal has to vary. In digital communication, bandwidth is expressed in bits per second (bps). In analog communications, bandwidth is expressed in cycles per second or hertz (hz). The speed limit in copper wire is determined by the nature of electric currents, while in optical fiber the speed limit is determined by its dispersion effects. Figure 9 compares the bandwidth capabilities of copper coaxial and optical fiber medium in terms of the attenuation factor *a*.

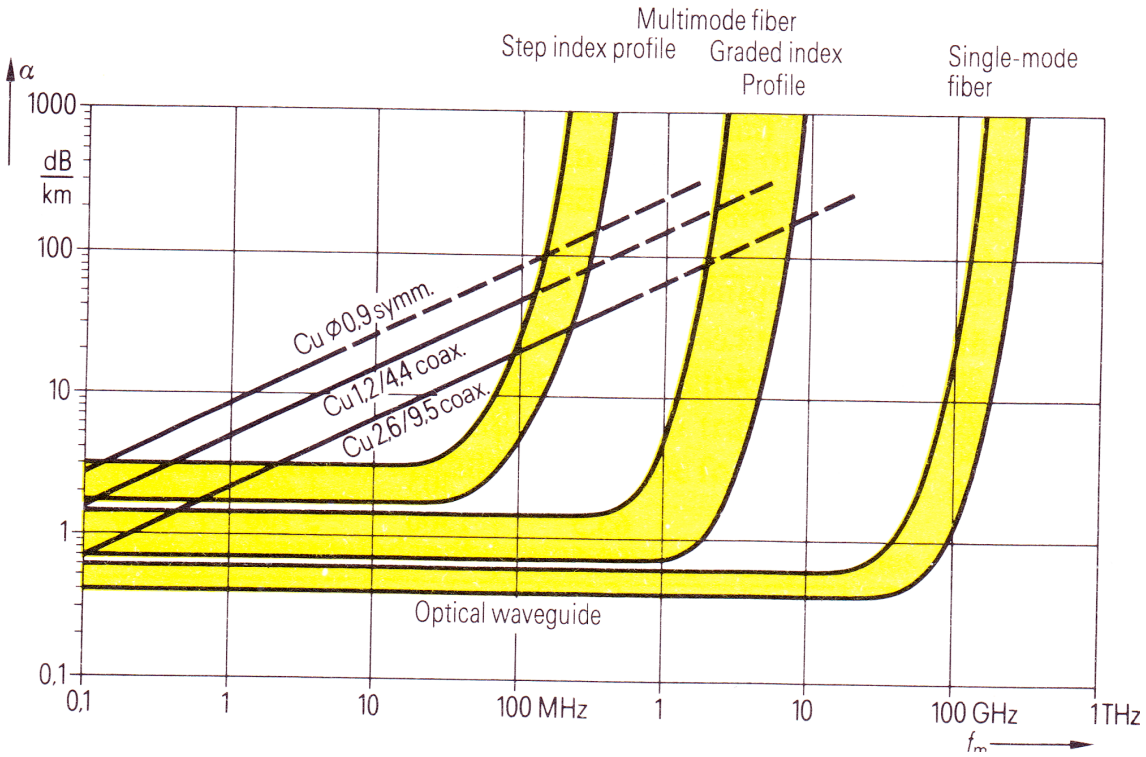

Figure 9: Copper coax vs. optical fiber bandwidth

1.3.2 Multiplexing

The need for multiplexing is driven by the fact that it is much more economical to transmit data at higher rates over a single fiber that it is to transmit at lower rates over multiple fibers[10], given of course that the bandwidth is available. Multiplexing is the sharing of a single channel's resources by more than one user. These resources can be time, frequency, and in the case of optics wavelength.

1.3.2.1 Time Division (TDM)

In Time Division Multiplexing (TDM) more than one user share the time resources of a single transmission channel. For example, 64 155Mb/s data streams can be multiplexed into a single 10 Gb/s capacity channel. This is done by assigning a specific time users can transmit data trough the shared channel, then cycling through each user for the allocated period of time.

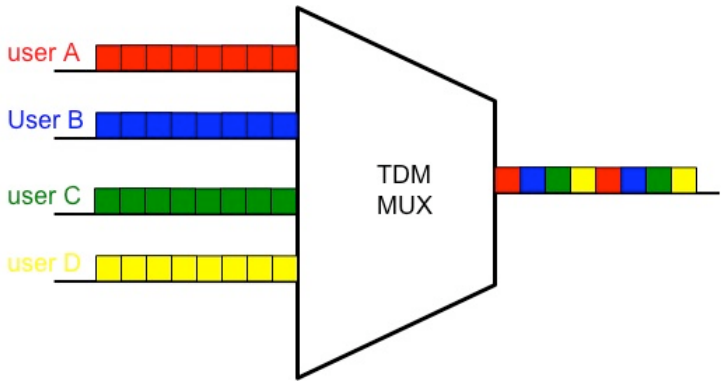

Figure 10: TDM

This multiplexing technique requires higher speed, more complex electronics and of course more bandwidth. Research is being conducted to execute TDM with optical components, which is known as optical time division multiplexing (OTDM). Laboratory experiments have demonstrated several 10Gb/s into a 250Gb/s optical channel.

1.3.2.2 Wave Division (WDM)

WDM is the optical equivalent of frequency division multiplexing for electronic communications. Like FDM, WDM assigns the data from each user to a specific *frequency*. In the case of optics the *frequency* corresponds to the *wavelength* or color of the light source used to transmit the data. Different users can transmit data using different colors through the same optical fiber at the same time. The number of different wavelengths supported by a single fiber, and therefore total data capacity, depends on the spectral composition of each color. The more

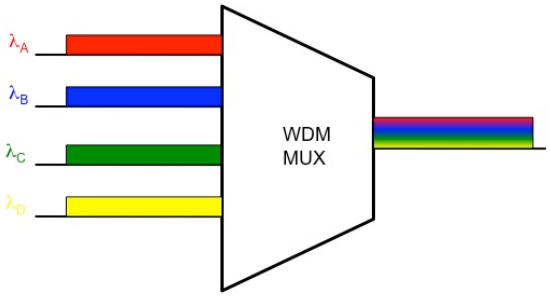

Figure 11: WDM

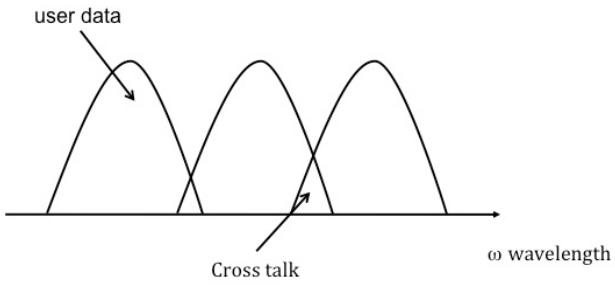

Figure 12: Channel spacing in WDM

pure, or coherent, a light source is, the closer together adjacent wavelengths can be without crossing over into the adjacent wavelength/channel.

1.3.2.3 Spread Spectrum

Spread spectrum (SS) multiplexing has been investigated extensively in the realms of satellite and mobile communication, and offer several advantages for access data networks. SS substantially increases the bandwidth occupied but the transmitted data. Because of fiber optics extremely high bandwidth capacity, SS as a multiplexing technique is highly attractive for high speed and communications. Since data in LANs and access networks are typically bursty, spread spectrum is a more suitable multiplexing technique compared to TDM, FDM, and WDM due to its asynchronous nature. SS provides asynchronous access to each user by allowing multiple

users to share the entire channel, as opposed to TDM or WDM where the users share a portion of the total channel capacity[2].

Code division multiple access (CDMA) is a form of spread spectrum multiplexing where data is assigned orthogonal codes for each bit sent, later to be decoded by correlation techniques only by the intended recipient of the data. To better elaborate, CDMA is accomplished by encoding each data bit of a stream with a unique logical identifier rather than a time or frequency, as in TDM and WDM respectively. After encoding, data from all the users of the network is transmitted over a single fiber. Armed with the knowledge of the codes used by several transmitters, a receiver extracts the desired user from all the other users by comparing the coded multiuser stream with a copy of the desired code and rejecting the codes that do not match[11]. This thesis concentrates on *incoherent* OCDMA, where the code representing data bits are unipolar (0,1) sequences. Auto- and cross-correlation operations are preformed in terms of optical intensity (optical power amplitude).

1.3.2.4 Passive Optical Networks (PON) and Fiber to the Home (FTTH)

The narrow bandwidth of copper wire reaching individual homes has long limited the service providers' ability to deliver telecommunications services to homes [8]. However, since the year 2000, telephone companies and real estate developers have installed fiber-to-the-home systems in new sub-divisions. The industry has developed a family of last mile optical network names "fiber to the X" (FTTx) that include the following:

- FTTB: *Fiber to the Business* (or sometimes, Fiber to the Building)
- FTTH: *Fiber to the Curb* (near homes, but not all the way to them)
- FTTD: *Fiber to the Desk*

- FTTH: *Fiber to the Home*
- FTTN: *Fiber to the Neighborhood* (or fiber to the Node).

This thesis the Fiber to the Home type access network is the one in question.

The *passive optical network* or PON design eliminates active optical components between the transmitting terminal and the end user/subscriber. Table 3 list important features of the three standards used in PONs [8].

Table 2: ITU Standards for PONs

Name	BPON(Broadband PON or Full Service Access Netowork)	GPON(Gigabit PON)	EPON(Ethernet PON)
Standard	ITU G.983	ITU G.984	IEEE 802.3 ah EFM
Data Packets	ATM	ATM or Ethernet	Ethernet
Downstream bandwidth	622 Mbits/sec	1.25 or 2.5 Gbits/sec	1.25 Gbits/sec
Upstream bandwidth	Total 155 or 622 Mbits/sec	Total 155 or 622 Mbits/sec or 1.25 or 2.5 Gbits/sec	1.25 Gbits/sec

2 LITERATURE REVIEW

The literature presented in this chapter spans the 20 years of continuing research on the application and development of CDMA as a multiplexing technique for fiber optic communications. The literature covers incoherent OCDMA fundamentals, beat noise, and Passive Optical Network (PON) and Fiber to the Home(FTTH) experimental deployments.

2.1 OCDMA Fundamental Principles

Code Division Multiple Access as applied to optical networks has it origins in the work titled "Spread Spectrum Fiber-Optic Local Area Network Using Optical Processing" submitted to the IEEE Journal of Lightwave Technology by P.R. Prucnal, M.A. Santoro, and T. Rui Fan [2]. It defines the use of orthogonal codes to address each user using optical fiber-delay lines. It concentrates on the use of Gold Codes to perform the auto- and crosscorrelation functions. The paper defines SNR in terms of number is users and autocorrelation function.

"Code Division Multiple Access...Part 1..." by J.A. Salehi [12] gives the definition of the Optical Orthogonal Codes used in this thesis and the criteria on their design. This work also goes on to define the correlation constraints for auto- and crosscorrelation in discrete time, which is how this thesis treats the analysis of the mathematical models for the encoding and decoding sections of the network. The work goes on to define probability density function for two interfering OOC codes. This is pertinent to future works presented by this thesis to design a proper threshold technique to detect the autocorrelation.

Part two of the paper by J.A. Salehi [13] takes the results of the OCDMA experiment using OOC and defines the BER according to the number of users and the level of the threshold

mechanism. It provides with the probability density function of the interference signal for N users. The work proposes the use of an optical hard limiter to reduce the signal intensity of the interfering users.

2.2 Beat Noise

In the work by T. Bazan, D. Harle, and I. Andonovic [14] titled "Interferometric Noise in Optical Code Division Multiple Access", the authors give an overview of the different types and classification of interferometric noise. Here, the impact of beat noise on time-wavelength OCDMA is evaluated and proves to be similar to the 1-D time-OCDMA experiment presented in this work.

"Analysis of Beat Noise in Coherent and Incoherent Time-Spreading OCDMA" [1] analyzes the effects of beat noise by defining the coherent ratio, which is the ratio of chip duration to the coherence time of the light source. This work mentions that averaging throughout the detection enables the noise analysis to ignore beat noise in incoherent OCDMA schemes. This leads to the proposal in this thesis of using the multimode fiber in the decoding stages.

In citation [15], "Analysis of Phase Noise of RF Signals in Analog Fiber Optic Systems" the author proposes an experimental setup for measuring phase noise in a fiber optic link. This is of some importance as the summation of the same wavelength at the decoding stages of our network cause the beat noise. The experiment presented measures phase in both the electric and optical domains, allowing to analyze the effects of adding optical components to the network.

2.3 PON and FTTH

The Evolution of PON-based FTTH solutions is described in the work [16] by K.S. Kim. The paper reviews and compares the current PON-based technologies as of 2003. It describes the advantages and disadvantages of TDM multiplexing protocols, APON and EPON and discusses the possible evolution to include WDM via Arrayed Waveguide Gratings (AWGs) and Waveguide Grating Routers (WGRs).

Kitayama, Wang, and Wada propose a gigabit symmetric FTTH topology using OCDMA over WDM PON in [17]. The work gives a system overview of all the effects of OCDMA. The coding technique of using superstructured fiber Bragg gratings (SSFBGs) via coherent OCDMA are beyond the scope of this research, however, it is a notable reference for the overall wide scale implementation of such a network.

3 METHODOLOGY

3.1 Network Configuration

The experimental network represents a FTTH topology where two terminal users are receiving data from a central service provider; this is similar to a cable television service topology where the data stream is sent one way to the end user. In conventional FTTH OCDMA networks the CDMA spreading and de-spreading are done via passive optical components. The experiment in this thesis performs the spreading with electronic components while performing the despreading in with passive optical components. This configuration is proposed as a solution to the cost of network expansion of FTTH PONs and the reduction of beat noise caused by optical OCDMA spreading via optical couplers.

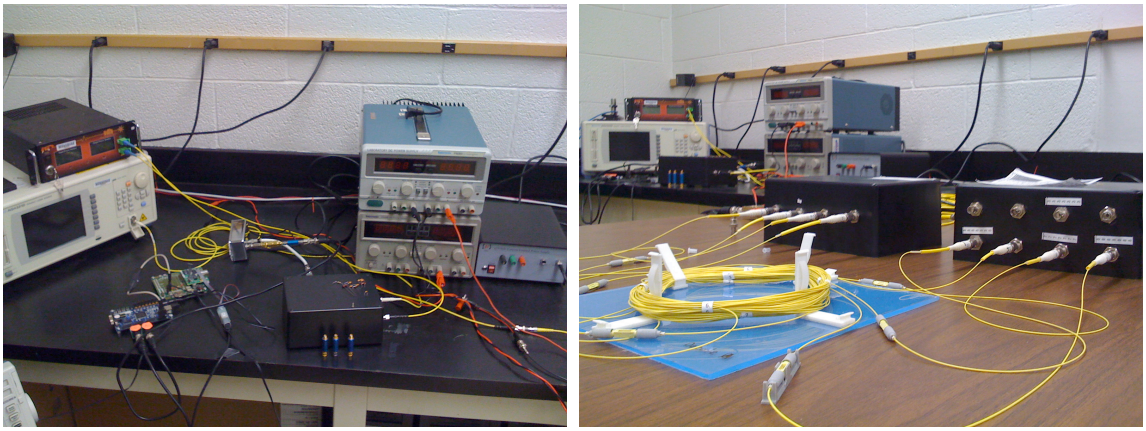

Figure 13: Experimental network topology physical implementation

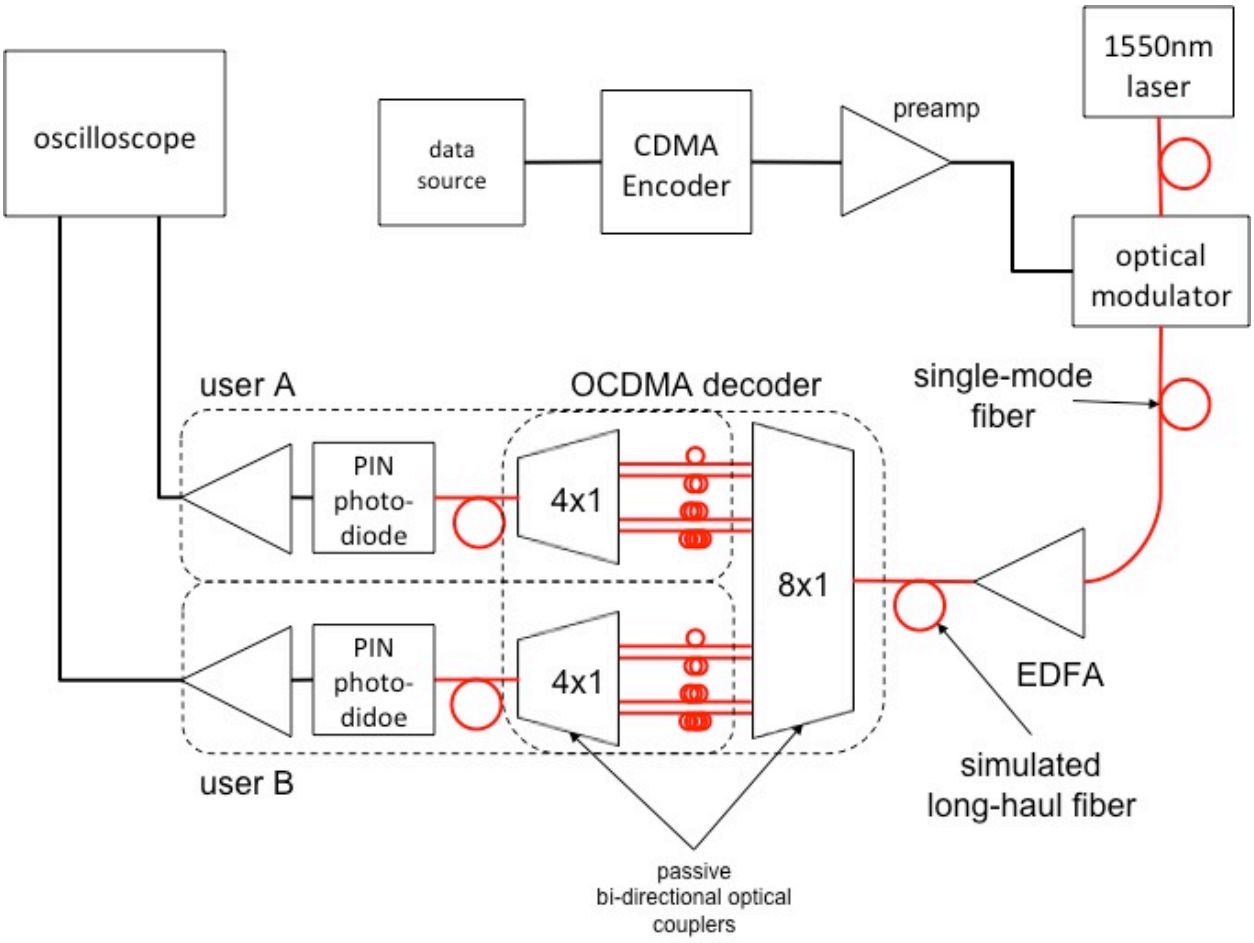

Figure 14: Experimental network topology diagram

The data source generates 1000 random 8-bit sequences at 118.2 Kbps using standard non-return-to-zero logic (NRZ). The CDMA encoder is a Field Programmable Array Logic (FPGA) package with an internal clock of 100Mhz. The NRZ data from the source triggers the generation of the CDMA codes on every rising edge of the every bit. The CDMA code is generated at 100Mhz. All the opto-electric devices are designed for a 50-W system, an isolation amplifier is needed to interface the FPGA to the optical modulator. The external optical modulator allows light to be transmitted with intensity proportional to the input electrical signal. The light source is a tunable variable frequency laser source that supplies constant laser light at the 1550 nm wavelength. All the optical fiber used in the experiment is single mode fiber. An

Erbium Doped Optical Amplifier (EDFA) is used before the decoding stage to over come the losses experienced by the bi-directional optical couplers. The CDMA decoding section is comprised of an 8x1, two 4x1 optical couplers, and 8 tuned fiber optic delay lines. The 8x1 coupler consolidates splitting the signal eight ways each with 1/8 of the optical power for both users without the need for extra optical components. Each user has an independent 4x1 coupler connected to the four specified delay lines for proper reception/rejection of the coded data bits. The 4x1 couplers add the optical power from all four legs into the one output to the PIN photoreceptor. A high gain RF amplifier follows the photoreceptor into an oscilloscope with 50W terminations for correlation peak detection and analysis.

3.2 Timing

The first positive bit of the data sequence from the source is periodic. The logic zeros preceding the first logic one of the sequence are ignored. This allows for easy detection and capture for analysis of the all waveforms associated with a data bit. In order to receive the proper data stream, a start bit will have to be amended to the beginning of each data word for synchronization and detection by the terminal user. Communication between the central station and the terminal users is asynchronous due to the nature of the temporal OCDMA coding.

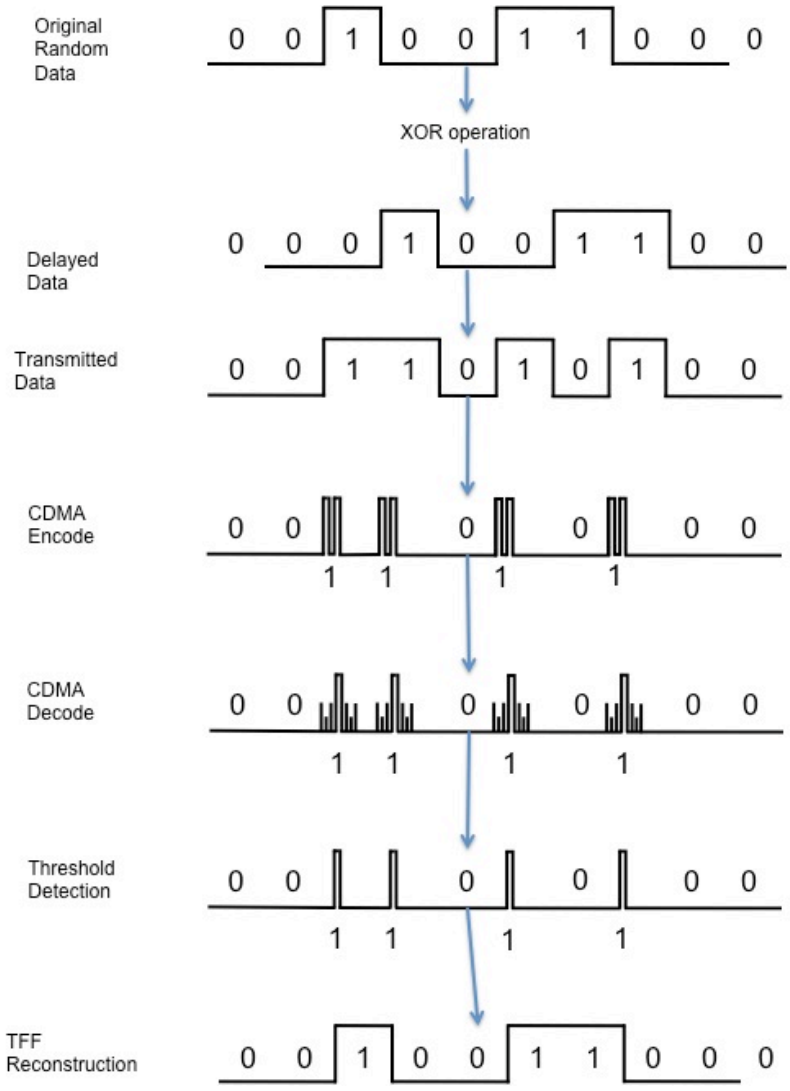

Figure 15: Time coding

Internal to the data source, each byte is delayed by one clock cycle then an exclusive OR operation is performed between the original and delayed byte sequences. The resulting byte from the logic operation is then transmitted through the network as described in the previous section of this chapter. Assuming the coded data produces a correlation peak, once it passes by its corresponding optical decoding sequence and threshold detection, each logic 1 bit is now represented by a sole *chip* approximately 10ns in width. At the user, each chip received triggers a change of state for a trigger flip-flop resulting in the *original* data sequence. With this

communication scheme, it is unnecessary to have a global synchronizing clock for the network. The data rate is dictated by the frequency of the correlation chips and not the global clock.

3.3 Incoherent OCDMA coding scheme

Optical Orthogonal Codes (OOCs) and prime codes are two well-known families of 1-D unipolar codes designed for incoherent OCDMA[18]. An (n,w,l_a,l_c) OOC is defined as a binary code C of length n, with a weight w. The weight is the number of "1s" in said sequence. The auto- and cross-correlation properties of an OCC compared to itself and other OOCs is given by the following[12]:

- Auto-correlation Constraint: For any $\mathrm{X}=[x_0,x_1,.....,x_{n-1}]\in C$ and any integer $\tau\in(0,n)$,

$$\sum_{t=0}^{n-1} X_t X_{t\oplus\tau} \geq \lambda_a$$ where "$\oplus$" denotes modulo-n addition

- Cross-correlation Constraint: For any $\mathrm{X}=[x_0,x_1,.....,x_{n-1}]\in C$ and any $Y=[y_0,y_1,.....,y_{n-1}]\in C$ such that $Y\neq X$ and any integer t,

$$\sum_{t=0}^{n-1} X_t y_{t\oplus\tau} \leq \lambda_c .$$

To reduce multi user interference, incoherent codes must be sparse in binary ones and have very low autocorrelation side lobes and cross-correlation functions. The experiment uses two (7,4,2,2) OOCs: $A=[1,1,0,0,1,1,0]$ and $B=[1,0,1,1,0,1,0]$. These code sequences were chosen as they exhibited *good* auto- and cross- correlation properties with each other.

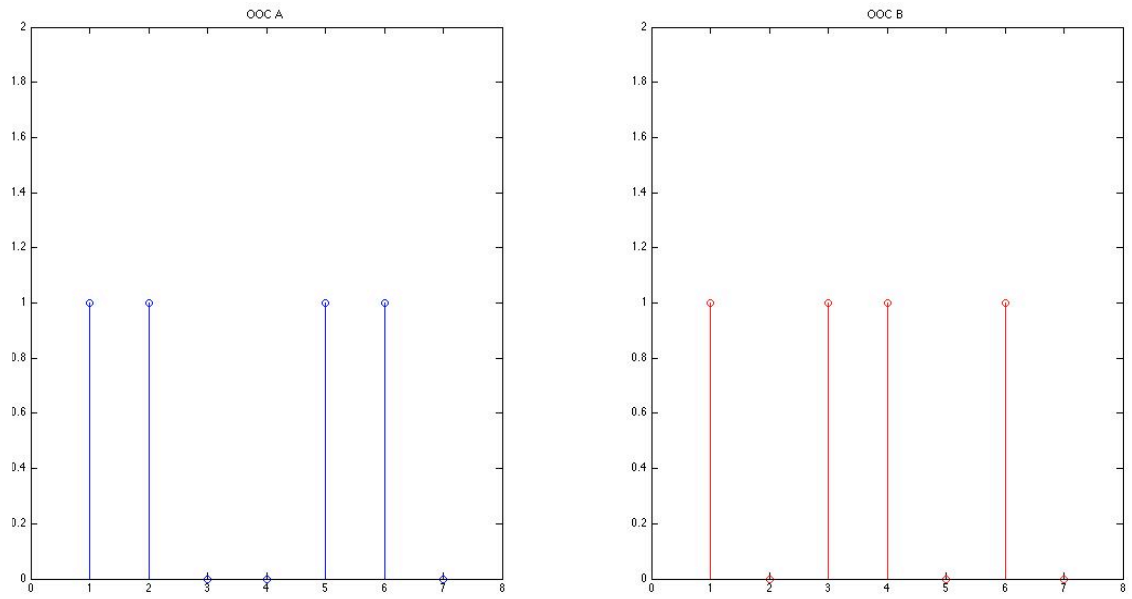

Figure 16: OOCs for users A and B

Figure 15 shows the temporal representation of the OOCs. Performing the auto- and cross correlation constraint algorithms is simply computing a circular convolution with each OOC to itself and between each different one respectively. Figure 16 shows the results of the correlation properties of the OOCs used in this experiment.

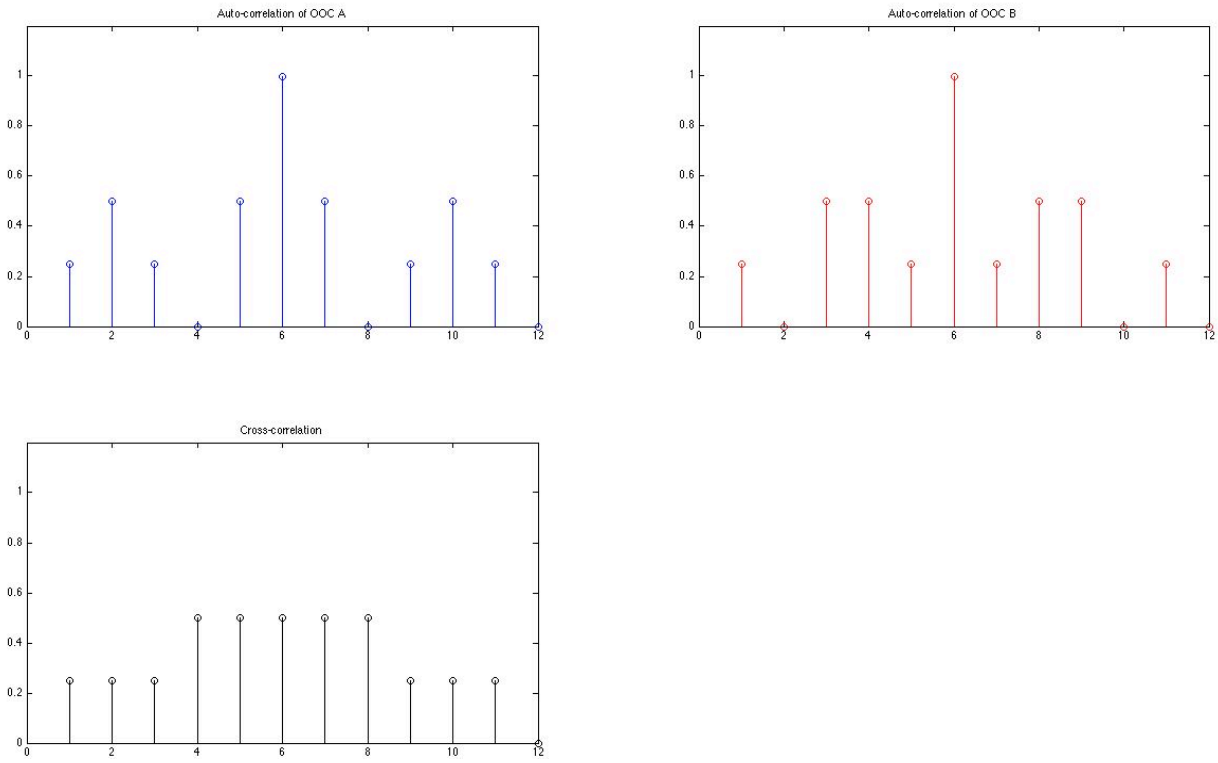

Figure 17: Auto- and cross-correlations of A and B codes

3.3.1 Experimental Implementation

OOCs A and B are physically implemented in the experiment two different ways: with 10ns bit width pulses generated by the FPGA upon the rising edge of each data bit and with optical delay lengths interconnected with passive couplers. Each optical delay is measured to exhibit a light propagation delay in incremental time portions of 10ns. The length of each delay line, is computed using equation (4). To realize the generation of each OOC and the auto- and cross- correlation algorithms using passive optics, one can consider the combination of optical couplers and delay lines as having an impulse response that is equal to the OOC desired. The number of coupler ports indicates the maximum weight *w* of the OOC code. The length of each fiber optic delay path dictates the position of each logic 1 in the sequence. This is depicted in figure 17. If the input x(t) is not an impulse, but one of the OOCs, this optical delay system

performs a convolution operation between the input OOC and the impulse response of said system.

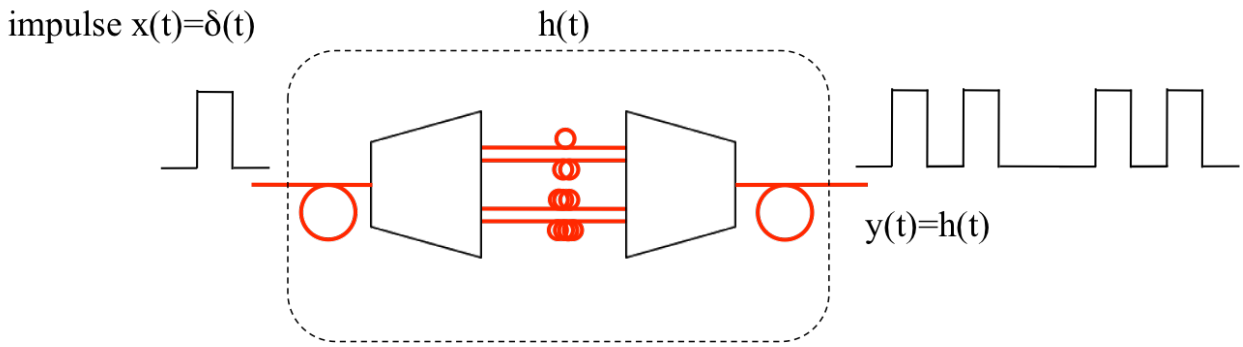

Figure 18: Optical delay line impulse response

The FPGA generates the unique OOC for each user and transmits it across the network, while the optical fiber delays perform the auto- and cross- correlation at each user. For example, the data encoded by the FPGA for user A, will produce a correlation peak for each bit similar to figure 16a when it reaches the optical delay decoding section for user A. This correlation peak can be detected by setting an appropriate threshold then translating the *chip* into a data bit as described in the previous section. When the same encoded information reaches user B's decoding section, it will produce a waveform similar to figure 16c, which in turn will result in no detection of a correlation peak and therefore no data.

4 EXPERIMENTAL RESULTS

The scope of this research is the ability to determine whether the end user of the optical network is able to receive data from a central terminal. In order to receive the data, the user must be able to detect a correlation peak produced by the passive optical components used to perform the OCDMA decoding function. Is this step, lies the analysis. Do the passive optical components generate a "strong" enough correlation peak for successful detection?

Referring back to figure 16 in Section 3.3; the mathematical implementation of the OCDMA decoding process shows a prominent correlation peak (for both codes A and B) at "time slot" 11. The amplitude of the correlation peaks are certainly greater than $l_a=l_c$, and are 2 times greater than the next highest value in the sequence. The cross-correlation result from both A and B decoding are the same due to the invertablility property of convolution and show that no value of the sequence is greater than l_c.

The waveforms presented in this chapter are comma-separated values (CSV) exported from the oscilloscope used in the network. "Snapshots" were taken of the data transmitted through the network. For this analysis we only look at the first "logic 1" bit from each 8 bit data word. There are a total of 24 snapshots taken. There are 6 samples of each correlation combination codec AA, codec BB, codec AB, and codec BA. "Codec" of course stands for "code/decode". Codecs AA and BB produce an auto-correlation while codecs AB and BA produce a cross-correlation. It is notable to mention that the cross-correlations between A and B both produce equal chip sequences. The CSV files were generated at a resolution of $5x10^9$ samples/sec with a total of $10x10^3$ samples per file. Figure 18 shows an example of one of the snapshots, this does not tell us much about the OCDMA coding, and so the data was cropped

from sample point 1200 to 2200 to show more detail (figure 19). The waveform in figure 19 is also easier to work with in Matlab as it only contains 1001 points as opposed to $10x10^3$.

The unipolar (0,1) incoherent structure of the OCDMA coding scheme dictates that the bit detection analysis is to be done in terms of amplitude or optical intensity; more specifically, the amplitude of the correlation peak, or lack there of, with respect to the amplitude of the other chips within the data sequence.

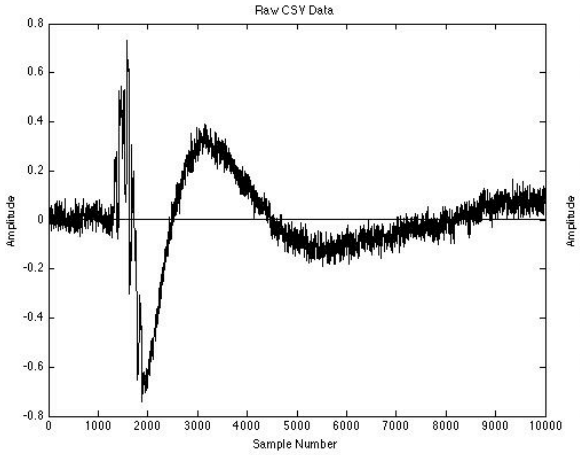

Figure 19: Raw CSV Data

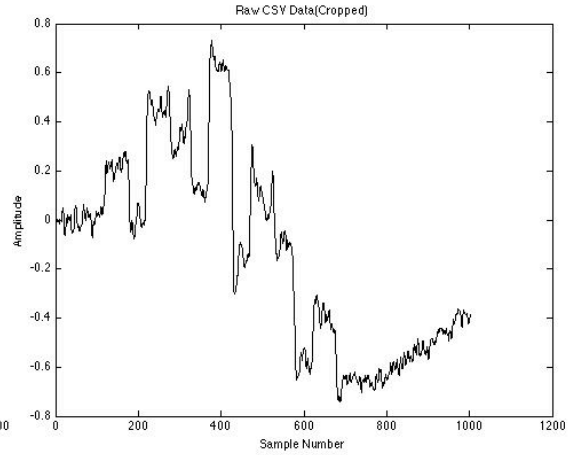

Figure 20: Raw CSV Data (Cropped)

The physical implementation of the network is based on a 50-W communications system, so capacitive and inductive effects of line impedance matching and amplifiers are unavoidable. Equalization of the various electronic and optical components in the network are beyond the scope of this research and are left for future work. This does not however, remove the problem of trying to analyze correlation results based on amplitude when the pertinent data exhibits a zero-reference shift caused by capacitive/inductive discharge as seen in figures 18 and 19. Fortunately, the distorted data resulting from the correlation operations do resemble the mathematical models in figure 16. The distortion does not affect the time values of the signal, only the amplitudes. As an example, if figure 19 is compared to figure 16, it is apparent that

figure 19 is the auto-correlation of B. This comparison alone is not enough to verify if the amplitude level of the correlation peak is sufficient enough for the user to detect only the one prominent chip in the sequence and therefore, reconstruct the original data sent by the central terminal.

4.1 Signal reconstruction via linear regression approximation

The method to remove the capacitive/inductive distortion imposed on the correlation data involves approximating the zero-amplitude level and shifting the waveform by the difference between the approximated zero-level and the x-axis origin. To elaborate, the amount of amplitude offset at each sample point can be determined by approximating the zero-level using known zero-values as points to construct a polynomial least squares fit. The zero values of each waveform are determined by comparing the sampled data to the mathematical model (figure 16). For the auto-correlation of A the reference values are located at time slots 0, 4, 8, and 11. For the auto-correlation of B the reference values are at 0, 2, 10, and 11. For the cross-correlations, the values are located at time slots 0 and 11.

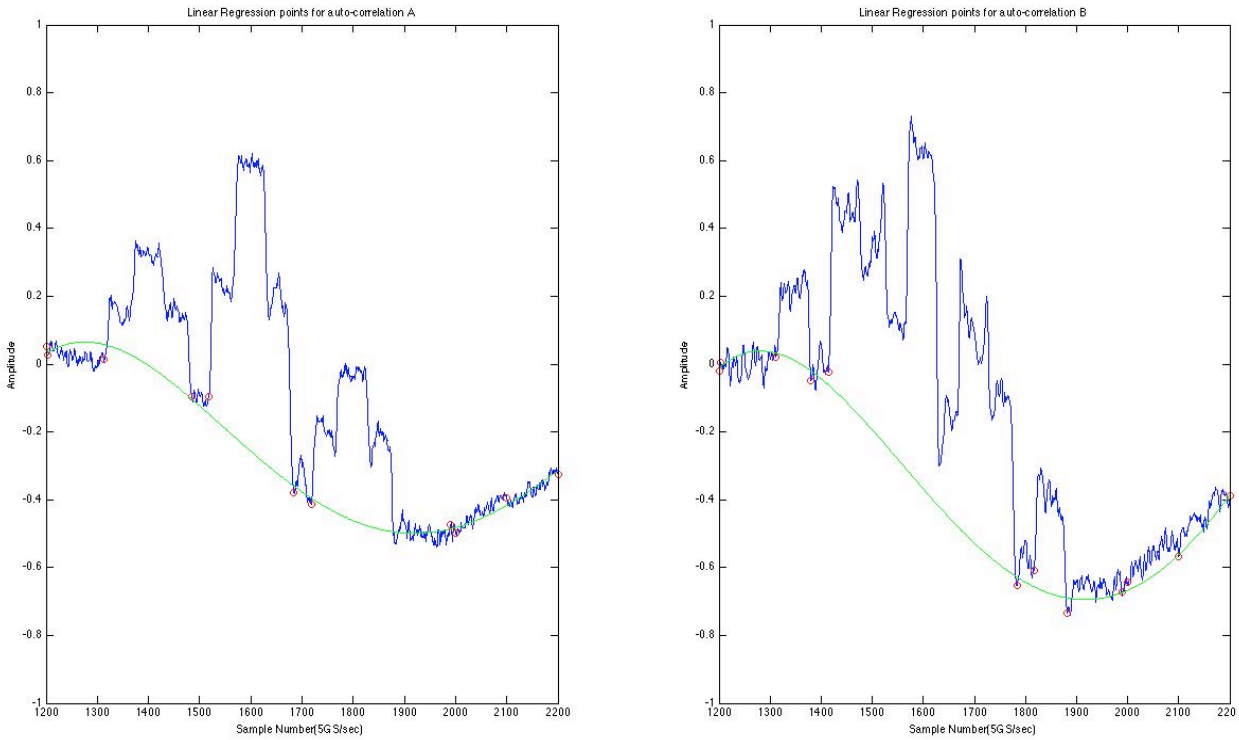

Figure 21: Polynomial zero level line fitting

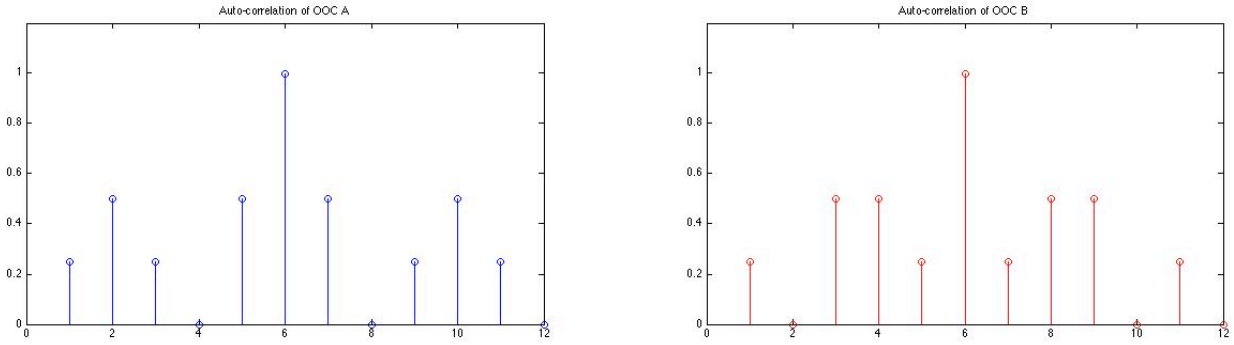

Figure 22: Zero reference level selection based on mathematical models

Once these points were defined for each correlation combination, both *polyfit* and *polyval* Matlab functions were used to construct the approximate zero reference level with a 4th order polynomial curve and evaluate the value of said polynomial at each sample point. This is shown in figure 20. At each sample point, the difference between the x-axis origin (0) and the evaluated polynomial value was added to the distorted signal resulting in a positive amplitude shift for

values found below the x-axis. This restored the zero reference level to the x-axis origin, removing any amplitude shift associated with capacitive and inductive distortion effects.

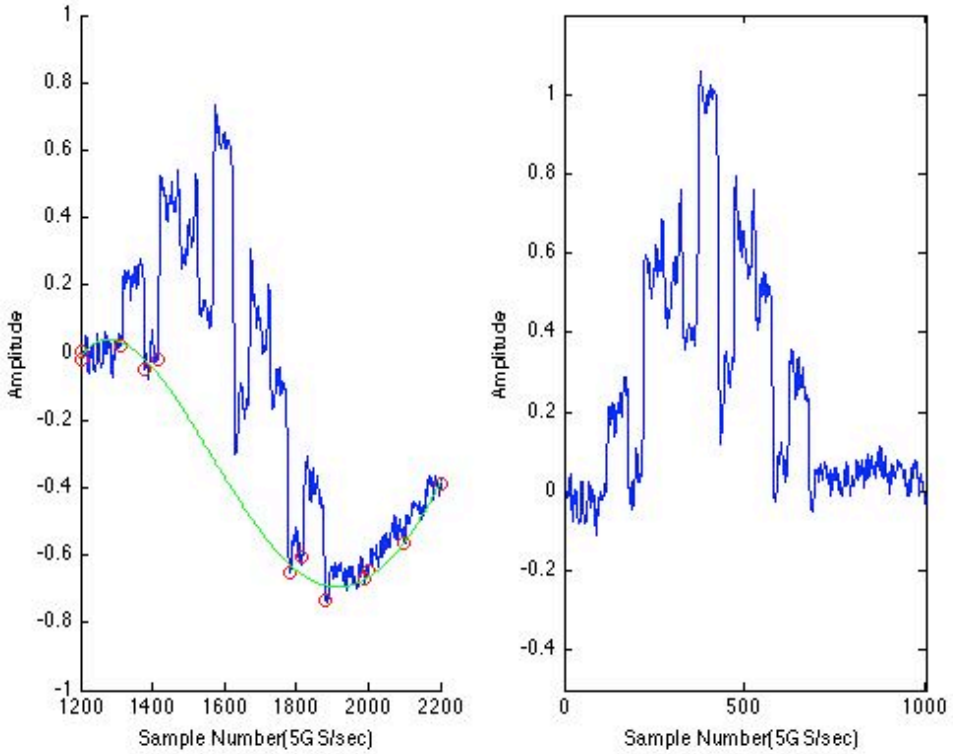

Figure 23: Auto-correlation B with zero level restoration

4.2 Correlation Peak Analysis

In order for the network user to successfully decode information multiplexed with incoherent OCDMA, the autocorrelation peak resulting from the optical delay line decoder must have an amplitude greater than any other peak in the autocorrelation code sequence. The autocorrelation peak must also be greater than the maximum amplitude of any peak in the crosscorrelation sequence. According to the correlation constraint equations presented in chapter 3, these values are defined as l_a and l_c. To successfully transmit information to a specific user the

autocorrelation peak must be greater than l_a for the intended user while the crosscorrelation amplitudes for all the other users must be less than or equal to l_c to avoid erroneous detection.

The experimental results in the following plots certainly prove that incoherent OCDMA via optical delay line decoding is a possible multiplexing technique to implement in FTTH access networks, however due to the nature of the coding there are many issue that prevent it's commercial implementation; more predominantly, optical beat noise. To compare the experimental waveforms to the mathematical model in reference to amplitudes and impulse/chip time slots; each impulse of the mathematical models can be related to the center of each chip in the waveform. Figure 23 displays two normalized plots. The black plot is the result of encoding A passing through the optical delay section with a characteristic impulse response A, while the red plot is the result of code A passing through the optical delay section with character impulse response B. These optical delay lines are connected to the photo-detectors for users A and B respectively (refer to figure 13).

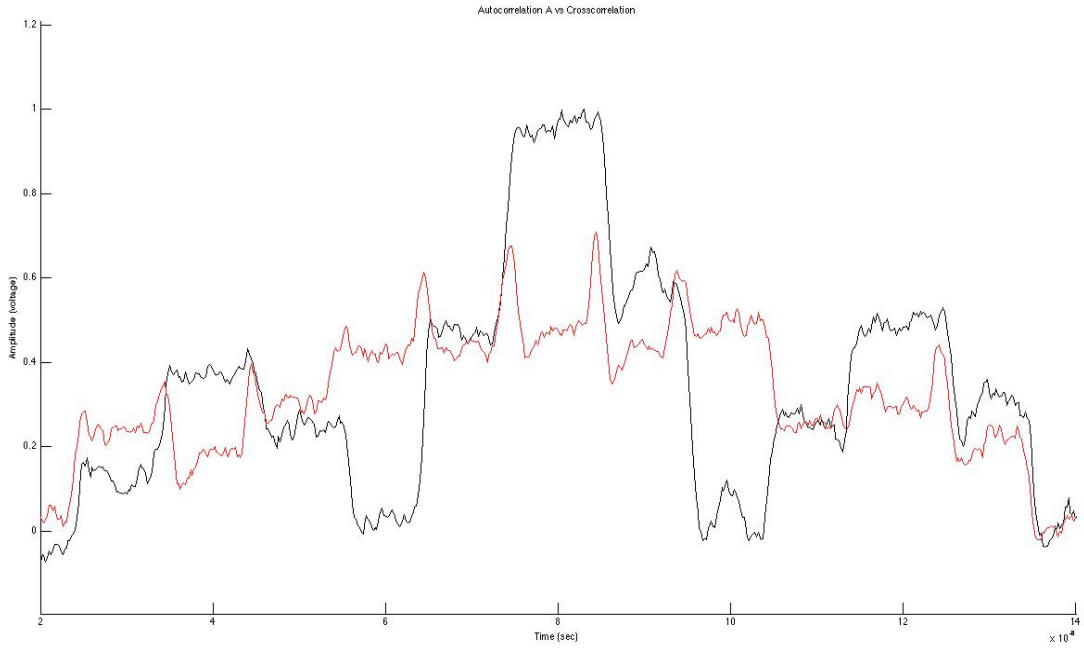

Figure 24: Autocorrelation A vs. crosscorrelation

It is clear that the information bit intended for user A exhibits the autocorrelation peak that is greater in normalized amplitude than $l_a=l_c=0.5$ for the OOC (7,4,2,2). The red plot indicates that no peak is greater than l_c. Therefore, the B user will not detect a peak above l_c and will not be able to reconstruct a bit of information. Each chip width in the sequence for both the auto- and cross-correlation waveforms measure approximately 11ns, which is consistent with proper the length of each individual optical delay line in the decoding sections and is consistent with the correlation peak being in the 6th time slot of the sequence.

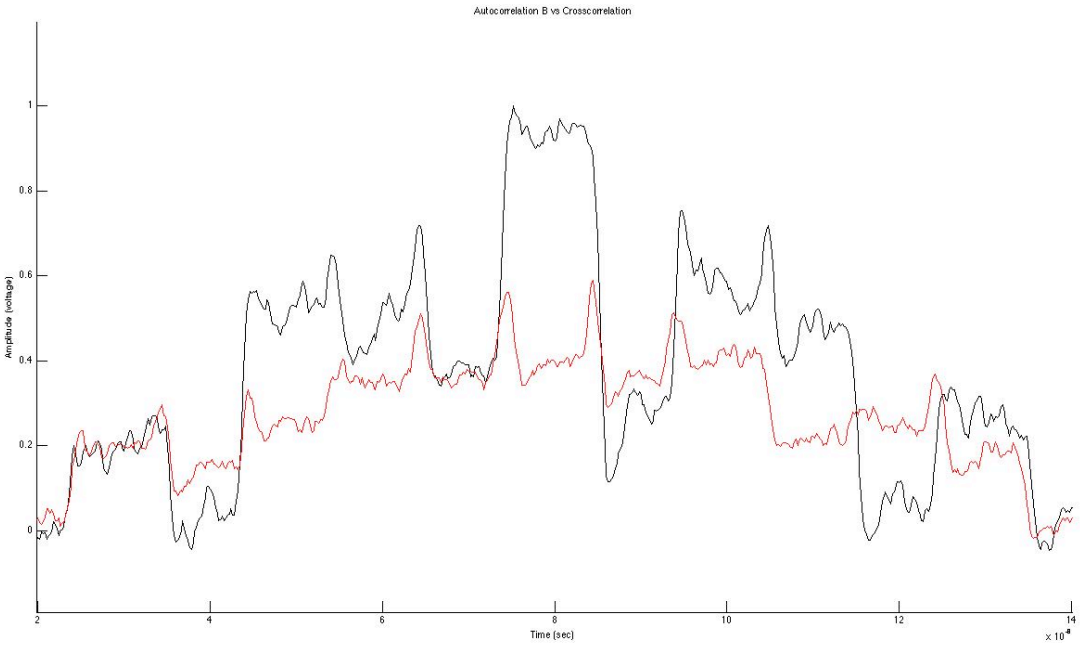

Figure 25: Autocorrelation B vs. crosscorrelation

Figure 24 shows the correlation results for the opposite configuration; where the central terminal transmits data intended for end user B and there encodes the information with OOC B. In this case, the results and analysis are similar to figure 23, here the normalized amplitude autocorrelation peak of B is 2 times greater than the other peaks in the autocorrelation sequence and all the peaks in the crosscorrelation chip sequence. When comparing the mathematical

model for autocorrelations and crosscorrelation to the experimental results, it is quite apparent that the relative amplitudes and time locations for each impulse and chip concur.

4.3 Decoder Interferometric Noise

One interesting phenomena of temporal coding using passive optics is what is known as Interferometric noise or beat noise. More destructive than interesting, this byproduct of OCDMA coding occurs when the same (delayed replicas) of different optical signals with identical or close to identical frequencies are incident simultaneously on the same photodetector [14], and is the major prohibitive factor to the wide scale implementation of this multiplexing technique. Figures 25, 26, and 27 in this section show the effects of beat noise on the decoded signals for A and B autocorrelations and crosscorrelation.

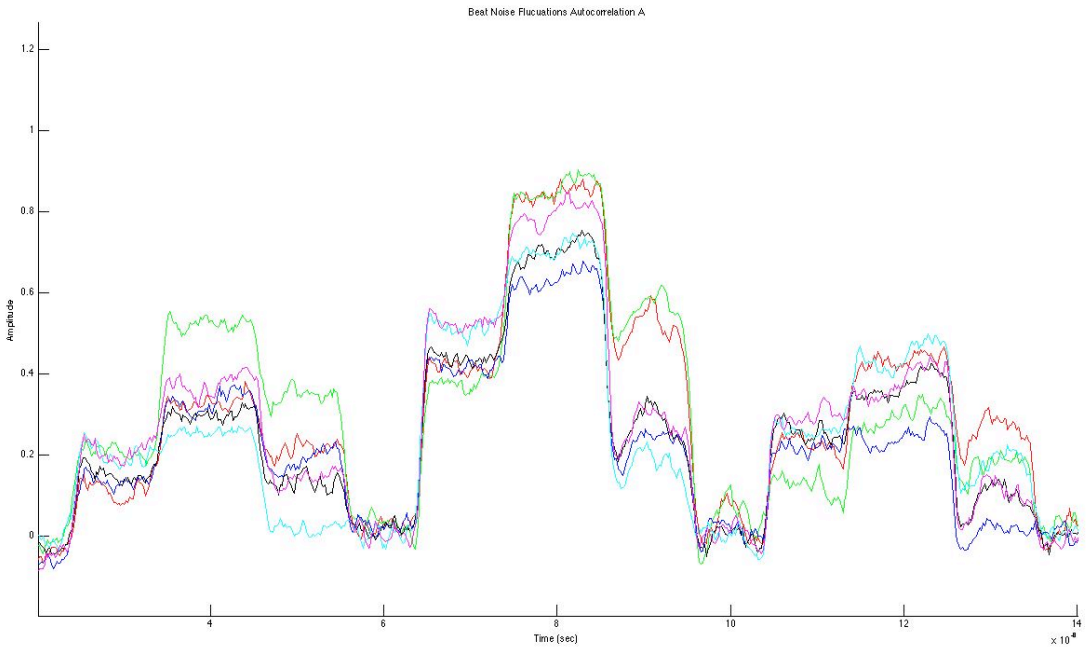

Figure 26: Beat noise fluctuations for autocorrelation A

Each color in the figure represents a sample snapshot of the A autocorrelation waveform. The characteristic shape of the autocorrelation still holds however the amplitudes at each point vary from snapshot to snapshot. Looking at a time point within the correlation peak (80ns) we see the amplitude varies up to 72.9% from the highest amplitude to the lowest, which is from two independent oscilloscope acquisitions. Looking at all three figures, beat noise only affects the amplitude of the signals and not the time displacement, from one acquisition to the next.

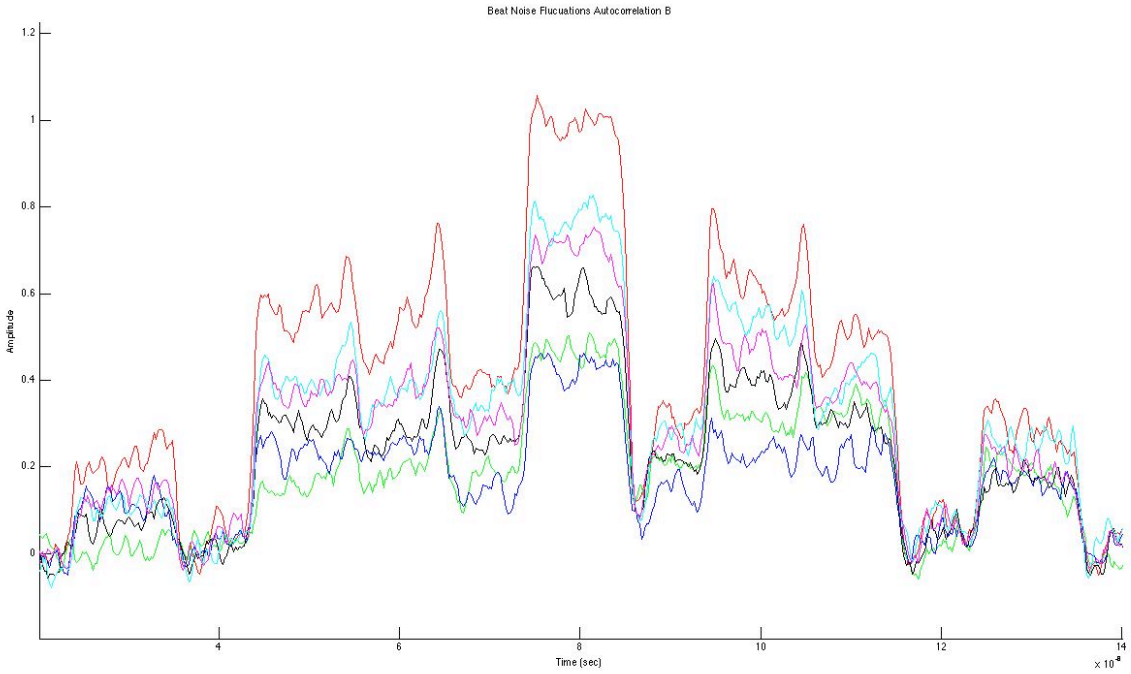

Figure 27: Beat noise fluctuations for autocorrelation B

To verify this, measuring pulse widths across the half amplitude of the autocorrelation peaks for all the OOC B samples yields a chip width of approximately $10.9e^{-9}$ sec. All the rise and fall values at the specified amplitudes are located in approximately the same time slots: 74.03 e^{-9} and 84.9 e^{-9} respectively. The autocorrelation B peak measurements for all the samples are listed in table 2.

Referring back to figure 14, the output of the optical decoding stage is introduced to a threshold mechanism; that, at predefined level preserves only amplitudes above the set level.

Theoretically, only the autocorrelation peak is persevered when passed through the threshold. Due to the beat noise experienced in the decoding stage, the delta in amplitude between different bits of information is too great for a static threshold level to properly preserve ONLY the autocorrelation peak [13].

Table 3: Autocorrelation B correlation peak chip width measurements

	Rising edge		Falling Edge			
Sample	Time Sample (ns)	Amplitude	Time Sample (ns)	Amplitude	Chip width (ns)	Amplitude Error
Blue	74.2	0.333	84.8	0.324	10.6	0.009
Green	73.8	0.338	85.0	0.327	11.2	0.011
Black	74.0	0.469	84.8	0.495	10.8	0.026
Magenta	74.0	0.499	85.0	0.534	11.0	0.035
Cyan	74.2	0.623	84.8	0.650	10.6	0.027
Red	74.0	0.775	85.0	0.731	11.0	0.044
				Average	**10.9**	**0.025**
				STD Dev	**0.2**	**0.014**

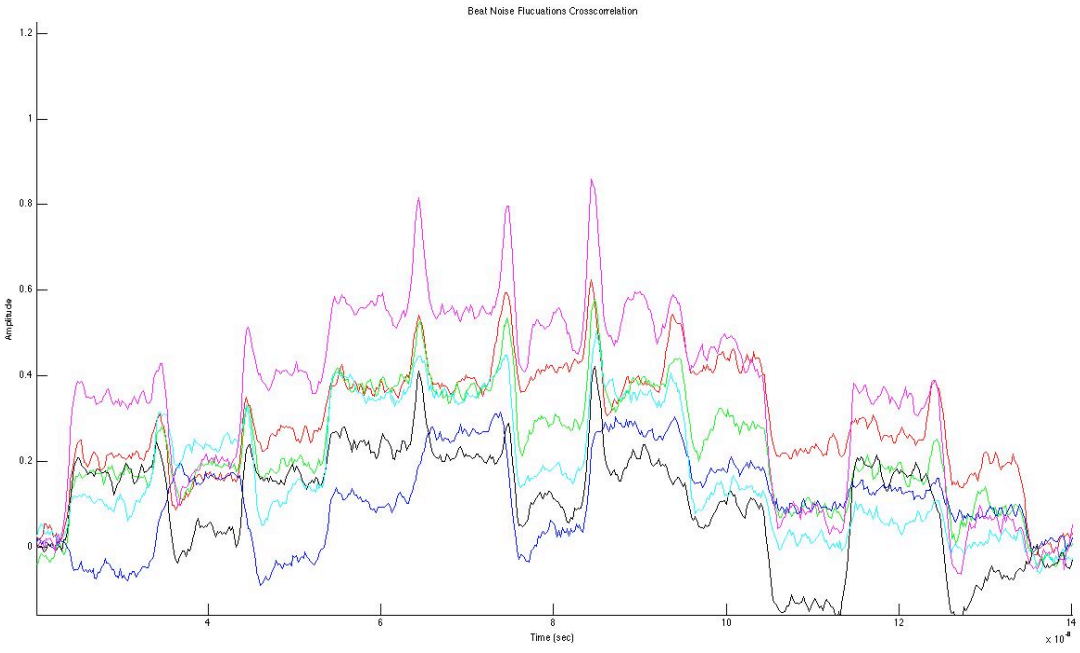

Figure 28: Beat noise fluctuations for crosscorrelation

5 CONCLUSION AND FUTURE WORK

The experiment presented in this thesis is based on incoherent OCDMA coding. There are many disadvantages to incoherent OCDMA, including small code size, low power and bandwidth efficiency, however it has been researched and is continued to be researched as a low cost method of multiplexing. As coherent OCDMA offers better performance it is prohibitably expensive to experiment much less deploy. This is why incoherent OCDMA is still being researched.

This work proved the ability to perform incoherent OCDMA encoding by electrical means while decoding via passive optical components. Why is this a leading research? The biggest problem with OCDMA PONs is scalability. As the number of users increases, so does the cost of expansion [16]. With the topology presented here, adding or dropping users is a matter of adapting software at the information source. At the user, expansion requires the assignment of an exclusive OOC and the use of inexpensive electrical and optical passive components. The expensive and sophisticated equipment lies at the central terminal, which can service many users dynamically. This FTTH network offers flexibility and low cost at reasonable performance. Early research has proven data rates of 100Mbs per user using the techniques. Which is far above data rates available today for consumer DSL or Cable Internet services.

5.1 Future Work

The experiment presented here made available many opportunities for future research. On a system level, the next steps are the equalization of waveforms, threshold design and bit

reconstruction, multiuser analysis, and data analysis. On a component level, the reduction of beat noise and optical nonlinearities.

There are many interfaces in the system, from digital CMOS voltages to 50-W line matching. Equalization of these electronic components according to each subsystem specification is important as distortion from these systems translates into the optical waveforms. The autocorrelation peak detection is a crucial portion of the system. Careful design of the mechanism is very important. One proposal is the design of a dynamic or moving threshold level, which fluctuates to follow the amplitude fluctuations caused by beat noise. It's important to analyze the network in terms of network data criteria, i.e. bit error rate, and eye patterns analysis. This provides with the information to quantify the performance of the network. It's well established that the major problem of this type of OCDMA PON is beat noise. There have been many method proposed to reduce the effects of beat noise on the system. We propose the use of multimode fiber optics in the decoding stage as a possible solution to reduce beat noise, and to the best of my knowledge this method has not been proposed. This idea lies on the premise that; the average optical power of all the propagation modes comprised of the encoded data at the center of the fiber's core (multimode core diameter is substantially greater than that of single mode) is greater than the average beat noise intensity change. Since we expect chip widths to be in the femto-second region for more advances incoherent OCDMA systems, multimode dispersion effects will have little to no effect on the chip decoding section, as the delay-line lengths are proportional to chip widths. A simple qualitative experiment was conducted at the University of Texas at El Paso to prove initial theories of this novel idea, which in fact did prove successful.

6 LIST OF REFERENCES

[1] X. Wang and K.-I. Kitayama, "Analysis of beat noise in coherent and incoherent time-spreading OCDMA," *Journal of Lightwave Technology,* vol. 22, pp. 2226-2235, 2004.

[2] P. Prucnal, M. Santoro, and F. Ting, "Spread spectrum fiber-optic local area network using optical processing," *Lightwave Technology, Journal of,* vol. 4, pp. 547-554, 1986.

[3] M. M. Karbassian, "Optical CDMA Networks," Birmingham: University of Birmingham, 2006.

[4] W. Stallings, *Data and Computer Communications*, 8th ed.: Pearson Prentice Hall, 2007.

[5] A. H. Cherin, *An Introduction to Optical Fibers*: McGraw-Hill, 1983.

[6] P. A. Tipler, *Physics for Scientist and Engineers*, 4th ed.: W.H. Freeman and Company, 1990.

[7] G. Mahlke and P. Gossing, *Fiber Optic Cables: Fundamentals, Cable Technology, & Installation Practice*. Berlin: John Wiley & Sons Ltd., 1987.

[8] J. Hecht, *Understanding Fiber Optics*, 5th ed.: Pearson Prentice Hall, 2006.

[9] J. C. Palais, *Fiber Optic Communications*, 5th ed. Upper Saddle River: Pearson Prentice Hall, 2005.

[10] R. Ramaswami and K. N. Sivarajan, *Optical Networks: A Practical Perspective*, 2nd ed.: Morgan Kaufmann, 2002.

[11] J. P. Heritage and A. M. Weiner, "Advances in Spectral Optical Code-Division Multiple-Access Communications," *Selected Topics in Quantum Electronics, IEEE Journal of,* vol. 13, pp. 1351-1369, 2007.

[12] J. A. Salehi, "Code division multiple-access techniques in optical fiber networks. I. Fundamental principles," *Communications, IEEE Transactions on,* vol. 37, pp. 824-833, 1989.

[13] J. A. Salehi and C. A. Brackett, "Code division multiple-access techniques in optical fiber networks. II. Systems performance analysis," *Communications, IEEE Transactions on,* vol. 37, pp. 834-842, 1989.

[14] T. Bazan, D. Harle, and I. Andonovic, "Interferometric noise in optical code division multiple access systems," in *International Conference on Transparent Optical Networks*, Nottingham, United Kingdom, 2006, pp. 97-100.

[15] C. Thomas, V. Gonzalez, A. Musa, and M. Shadaram, "Analysis of Phase noise of RF signals in Analog Fiber Optic Systems," in *Sarnoff Symposium, 2006 IEEE*, 2006, pp. 1-6.

[16] K. Kyeong Soo, "On the evolution of PON-based FTTH solutions," *Inf. Sci. Inf. Comput. Sci.,* vol. 149, pp. 21-30, 2003.

[17] K.-I. Kitayama, X. Wang, and N. Wada, "OCDMA over WDM PON - Solution path to gigabit-symmetric FTTH," *Journal of Lightwave Technology,* vol. 24, pp. 1654-1662, 2006.

[18] P. R. Prucnal, *Optical Code Division Multiple Access: Funamentals and Applications*: Taylor & Francis, 2006.

7 APPENDIX

7.1 OCDMA Encoder on FPGA software code

```
// Joel Quintana's Encoder
module encode (
                clk,
                reset,
                data_in,
                data_out);

input            clk_in;
input            reset;
input            data_in;
output           data_out;


reg [7:0]        counter;
reg              data_out;
reg              data_in_reg1;
reg              data_in_reg2;
wire             clk;                          // doubled clock from DLL
wire             idle = (counter == 0);

always @(posedge clk)  data_in_reg1 <= data_in;        // synchronizer for asynch signal
always @(posedge clk)  data_in_reg2 <= data_in_reg1;   // synchronizer for asynch signal

always @(posedge clk)
           if (reset)              counter      <= 0;            // reset
           else if (data_in_reg2)  counter      <= 1;            // start
           else if (!idle)         counter      <= counter + 1;  // count
           else                    counter      <= counter;      // hold

always @(counter)
           case (counter)
                0:          data_out = 0;
                1:          data_out = 0;
                2:          data_out = 1;
                3:          data_out = 0;
                4:          data_out = 0;
                5:          data_out = 0;
                6:          data_out = 1;
                7:          data_out = 0;
```

```
            default:      data_out = 0
        endcase


// this is a xilinx primitive and can double the frequency of the clkin
// at the clk2x output.    The clks will not be rising edge aligned.
// check xilinx docs for details - google "clkdll xilinx primitives"
CLKDLL dll (
                .CLKIN   (src_clk2       ),
                .CLKFB   (CLK0           ),
                .RST     (reset          ),
                .CLK0    (CLK0_dll       ),
                .CLK90   (               ),
                .CLK180  (               ),
                .CLK270  (               ),
                .CLK2X   (src_clk_fast   ),
                .CLKDV   (               ),
                .LOCKED  (               ));

endmoudule
```

7.2 Zero reference level reconstruction on Matlab

```
%Reading Raw CSV data from oscilloscope 6 samples for each correlation configuration
%-------------------------------------------------------------------------
AA_1=csvread('AA_1.CSV');  AA1=AA_1(:,2);
AA_2=csvread('AA_2.CSV');  AA2=AA_2(:,2);
AA_3=csvread('AA_3.CSV');  AA3=AA_3(:,2);
AA_4=csvread('AA_4.CSV');  AA4=AA_4(:,2);
AA_5=csvread('AA_5.CSV');  AA5=AA_5(:,2);
AA_6=csvread('AA_6.CSV');  AA6=AA_6(:,2);

BB_1=csvread('BB_1.CSV');  BB1=BB_1(:,2);
BB_2=csvread('BB_2.CSV');  BB2=BB_2(:,2);
BB_3=csvread('BB_3.CSV');  BB3=BB_3(:,2);
BB_4=csvread('BB_4.CSV');  BB4=BB_4(:,2);
BB_5=csvread('BB_5.CSV');  BB5=BB_5(:,2);
BB_6=csvread('BB_6.CSV');  BB6=BB_6(:,2);

AB_1=csvread('AB_1.CSV');  AB1=AB_1(:,2);
AB_2=csvread('AB_2.CSV');  AB2=AB_2(:,2);
AB_3=csvread('AB_3.CSV');  AB3=AB_3(:,2);
AB_4=csvread('AB_4.CSV');  AB4=AB_4(:,2);
AB_5=csvread('AB_5.CSV');  AB5=AB_5(:,2);
AB_6=csvread('AB_6.CSV');  AB6=AB_6(:,2);

BA_1=csvread('BA_1.CSV');  BA1=BA_1(:,2);
```

```
BA_2=csvread('BA_2.CSV');  BA2=BA_2(:,2);
BA_3=csvread('BA_3.CSV');  BA3=BA_3(:,2);
BA_4=csvread('BA_4.CSV');  BA4=BA_4(:,2);
BA_5=csvread('BA_5.CSV');  BA5=BA_5(:,2);
BA_6=csvread('BA_6.CSV');  BA6=BA_6(:,2);


%Linear Regression Operations to remove capacitive component from data
%and plots for Auto- and Cross-correlations A
%-------------------------------------------------------------------------
xa1=[1200 1203 1312 1485 1517 1684 1719 1990 2000 2100 2200];
ya1=[AA1(1200) AA1(1203) AA1(1312) AA1(1485) AA1(1517) AA1(1684) AA1(1719) AA1(1990) AA1(2000)
AA1(2100) AA1(2200)];          %
p1=polyfit(xa1,ya1,4);
Xa1=1200:2200;
Ya1=polyval(p1,Xa1);                                                    % Auto-correlation 1
for i=1:length(Ya1)
      Yad1(i)=0-Ya1(i);
      shiftAA1(i)=AA1(i+1199)+Yad1(i);
      transAA1=transpose(shiftAA1);
end

xxa1=[1200 1207 1313 1879 1990 2000 2100 2200];
yya1=[AB1(1200) AB1(1207) AB1(1313) AB1(1879) AB1(1990) AB1(2000) AB1(2100) AB1(2200)];
pp1=polyfit(xxa1,yya1,3);
XXa1=1200:2200;
YYa1=polyval(pp1,XXa1);                                  % Cross-correlation 1
for i=1:length(YYa1)
      YYad1(i)=0-YYa1(i);
      shiftAB1(i)=AB1(i+1199)+YYad1(i);
      transAB1=transpose(shiftAB1);
end

xa2=[1200 1203 1312 1485 1517 1684 1719 1990 2000 2100 2200];
ya2=[AA2(1200) AA2(1203) AA2(1312) AA2(1485) AA2(1517) AA2(1684) AA2(1719) AA2(1990) AA2(2000)
AA2(2100) AA2(2200)];          %
p2=polyfit(xa2,ya2,4);
Xa2=1200:2200;
Ya2=polyval(p2,Xa2);                                                    % Auto-correlation 2
for i=1:length(Ya2)
      Yad2(i)=0-Ya2(i);
      shiftAA2(i)=AA2(i+1199)+Yad2(i);
      transAA2=transpose(shiftAA2);
end

xxa2=[1200 1207 1313 1879 1990 2000 2100 2200];
yya2=[AB2(1200) AB2(1207) AB2(1313) AB2(1879) AB2(1990) AB2(2000) AB2(2100) AB2(2200)];
pp2=polyfit(xxa2,yya2,3);
XXa2=1200:2200;
YYa2=polyval(pp2,XXa2);                                  % Cross-correlation 2
for i=1:length(YYa2)
      YYad2(i)=0-YYa2(i);
      shiftAB2(i)=AB2(i+1199)+YYad2(i);
      transAB2=transpose(shiftAB2);
end
```

```
xa3=[1200 1203 1312 1485 1517 1684 1719 1990 2000 2100 2200];
ya3=[AA3(1200) AA3(1203) AA3(1312) AA3(1485) AA3(1517) AA3(1684) AA3(1719) AA3(1990) AA3(2000)
AA3(2100) AA3(2200)];
p3=polyfit(xa3,ya3,4);
Xa3=1200:2200;
Ya3=polyval(p3,Xa3);                                                    % Auto-correlation 3
for i=1:length(Ya3)
      Yad3(i)=0-Ya3(i);
      shiftAA3(i)=AA3(i+1199)+Yad3(i);
      transAA3=transpose(shiftAA3);
end

xxa3=[1200 1207 1313 1879 1990 2000 2100 2200];
yya3=[AB3(1200) AB3(1207) AB3(1313) AB3(1879) AB3(1990) AB3(2000) AB3(2100) AB3(2200)];
pp3=polyfit(xxa3,yya3,3);
XXa3=1200:2200;
YYa3=polyval(pp3,XXa3);                                    % Cross-correlation 3
for i=1:length(YYa3)
      YYad3(i)=0-YYa3(i);
      shiftAB3(i)=AB3(i+1199)+YYad3(i);
      transAB3=transpose(shiftAB3);
end

xa4=[1200 1203 1312 1485 1517 1684 1719 1990 2000 2100 2200];
ya4=[AA4(1200) AA4(1203) AA4(1312) AA4(1485) AA4(1517) AA4(1684) AA4(1719) AA4(1990) AA4(2000)
AA4(2100) AA4(2200)];      %
p4=polyfit(xa4,ya4,4);
Xa4=1200:2200;
Ya4=polyval(p4,Xa4);

% Auto-correlation 4
for i=1:length(Ya4)
      Yad4(i)=0-Ya4(i);
      shiftAA4(i)=AA4(i+1199)+Yad4(i);
      transAA4=transpose(shiftAA4);
end

xxa4=[1200 1207 1313 1879 1990 2000 2100 2200];
yya4=[AB4(1200) AB4(1207) AB4(1313) AB4(1879) AB4(1990) AB4(2000) AB4(2100) AB4(2200)];
pp4=polyfit(xxa4,yya4,4);
XXa4=1200:2200;
YYa4=polyval(pp4,XXa4);                                    % Cross-correlation 4
for i=1:length(YYa4)
      YYad4(i)=0-YYa4(i);
      shiftAB4(i)=AB4(i+1199)+YYad4(i);
      transAB4=transpose(shiftAB4);
end

xa5=[1200 1203 1312 1485 1517 1684 1719 1990 2000 2100 2200];
ya5=[AA5(1200) AA5(1203) AA5(1312) AA5(1485) AA5(1517) AA5(1684) AA5(1719) AA5(1990) AA5(2000)
AA5(2100) AA5(2200)];
p5=polyfit(xa5,ya5,4);
Xa5=1200:2200;
Ya5=polyval(p5,Xa5);                                                    % Auto-correlation 5
```

```
for i=1:length(Ya5)
    Yad5(i)=0-Ya5(i);
    shiftAA5(i)=AA5(i+1199)+Yad5(i);
    transAA5=transpose(shiftAA5);
end

xxa5=[1200 1207 1313 1879 1990 2000 2100 2200];
yya5=[AB5(1200) AB5(1207) AB5(1313) AB5(1879) AB5(1990) AB5(2000) AB5(2100) AB5(2200)];
pp5=polyfit(xxa5,yya5,3);
XXa5=1200:2200;
YYa5=polyval(pp5,XXa5);                                    % Cross-correlation 5
for i=1:length(YYa5)
    YYad5(i)=0-YYa5(i);
    shiftAB5(i)=AB5(i+1199)+YYad5(i);
    transAB5=transpose(shiftAB5);
end

xa6=[1200 1203 1312 1485 1517 1684 1719 1990 2000 2100 2200];
ya6=[AA6(1200) AA6(1203) AA6(1312) AA6(1485) AA6(1517) AA6(1684) AA6(1719) AA6(1990) AA6(2000)
AA6(2100) AA6(2200)];      %
p6=polyfit(xa6,ya6,4);
Xa6=1200:2200;
Ya6=polyval(p6,Xa6);                                       % Auto-correlation 6
for i=1:length(Ya6)
    Yad6(i)=0-Ya6(i);
    shiftAA6(i)=AA6(i+1199)+Yad6(i);
    transAA6=transpose(shiftAA6);
end

xxa6=[1200 1207 1313 1879 1990 2000 2100 2200];
yya6=[AB6(1200) AB6(1207) AB6(1313) AB6(1879) AB6(1990) AB6(2000) AB6(2100) AB6(2200)];     %
pp6=polyfit(xxa6,yya6,3);
XXa6=1200:2200;
YYa6=polyval(pp6,XXa6);                                    % Cross-correlation 6
for i=1:length(YYa6)
    YYad6(i)=0-YYa6(i);
    shiftAB6(i)=AB6(i+1199)+YYad6(i);
    transAB6=transpose(shiftAB6);
end



%Linear Regression Operations to remove capacitive component from data
%and plots for Auto- and Cross-correlations B
%-------------------------------------------------------------------------
xb1=[1200 1203 1312 1380 1414 1783 1817 1882 1990 2000 2100 2200];
yb1=[BB1(1200) BB1(1203) BB1(1312) BB1(1380) BB1(1414) BB1(1783) BB1(1817) BB1(1882) BB1(1990)
BB1(2000) BB1(2100) BB1(2200)];  %
p1=polyfit(xb1,yb1,4);
Xb1=1200:2200;
Y1=polyval(p1,Xb1);                                        % Auto-correlation 1
for i=1:length(Y1)
    Yd1(i)=0-Y1(i);
    shiftBB1(i)=BB1(i+1199)+Yd1(i);
    transBB1=transpose(shiftBB1);
```

```
end

xxb1=[1200 1207 1313 1879 1990 2000 2100 2200];
yyb1=[BA1(1200) BA1(1207) BA1(1313) BA1(1879) BA1(1990) BA1(2000) BA1(2100) BA1(2200)];      %
pp1=polyfit(xxb1,yyb1,3);
XXb1=1200:2200;
YYb1=polyval(pp1,XXb1);                                          % Cross-correlation 1
for i=1:length(YYb1)
      YYbd1(i)=0-YYb1(i);
      shiftBA1(i)=BA1(i+1199)+YYbd1(i);
      transBA1=transpose(shiftBA1);
end

xb2=[1200 1203 1312 1380 1414 1783 1817 1882 1990 2000 2100 2200];
yb2=[BB2(1200) BB2(1203) BB2(1312) BB2(1380) BB2(1414) BB2(1783) BB2(1817) BB2(1882) BB2(1990)
BB2(2000) BB2(2100) BB2(2200)];   %
p2=polyfit(xb2,yb2,4);
Xb2=1200:2200;
Y2=polyval(p2,Xb2);                                                  % Auto-correlation 2
for i=1:length(Y2)
      Yd2(i)=0-Y2(i);
      shiftBB2(i)=BB2(i+1199)+Yd2(i);
      transBB2=transpose(shiftBB2);
end

xxb2=[1200 1207 1313 1879 1990 2000 2100 2200];
yyb2=[BA2(1200) BA2(1207) BA2(1313) BA2(1879) BA2(1990) BA2(2000) BA2(2100) BA2(2200)];
pp2=polyfit(xxb2,yyb2,3);
XXb2=1200:2200;
YYb2=polyval(pp2,XXb2);                                          % Cross-correlation 2
for i=1:length(YYb2)
      YYbd2(i)=0-YYb2(i);
      shiftBA2(i)=BA2(i+1199)+YYbd2(i);
      transBA2=transpose(shiftBA2);
end

xb3=[1200 1203 1312 1380 1414 1783 1817 1882 1990 2000 2100 2200];
yb3=[BB3(1200) BB3(1203) BB3(1312) BB3(1380) BB3(1414) BB3(1783) BB3(1817) BB3(1882) BB3(1990)
BB3(2000) BB3(2100) BB3(2200)];   %
p3=polyfit(xb3,yb3,4);
Xb3=1200:2200;
Y3=polyval(p3,Xb3);                                                  % Auto-correlation 3
for i=1:length(Y3)
      Yd3(i)=0-Y3(i);
      shiftBB3(i)=BB3(i+1199)+Yd3(i);
      transBB3=transpose(shiftBB3);
end

xxb3=[1200 1207 1313 1879 1990 2000 2100 2200];
yyb3=[BA3(1200) BA3(1207) BA3(1313) BA3(1879) BA3(1990) BA3(2000) BA3(2100) BA3(2200)];
pp3=polyfit(xxb3,yyb3,3);
XXb3=1200:2200;
YYb3=polyval(pp3,XXb3);                                          % Cross-correlation 3
for i=1:length(YYb3)
      YYbd3(i)=0-YYb3(i);
```

```
    shiftBA3(i)=BA3(i+1199)+YYbd3(i);
    transBA3=transpose(shiftBA3);
end

xb4=[1200 1203 1312 1380 1414 1783 1817 1882 1990 2000 2100 2200];
yb4=[BB4(1200) BB4(1203) BB4(1312) BB4(1380) BB4(1414) BB4(1783) BB4(1817) BB4(1882) BB4(1990)
BB4(2000) BB4(2100) BB4(2200)];  %
p4=polyfit(xb4,yb4,4);
Xb4=1200:2200;
Y4=polyval(p4,Xb4);                                          % Auto-correlation 4
for i=1:length(Y4)
    Yd4(i)=0-Y4(i);
    shiftBB4(i)=BB4(i+1199)+Yd4(i);
    transBB4=transpose(shiftBB4);
end

xxb4=[1200 1207 1313 1879 1990 2000 2100 2200];
yyb4=[BA4(1200) BA4(1207) BA4(1313) BA4(1879) BA4(1990) BA4(2000) BA4(2100) BA4(2200)];    %
pp4=polyfit(xxb4,yyb4,4);
XXb4=1200:2200;
YYb4=polyval(pp4,XXb4);                                  % Cross-correlation 4
for i=1:length(YYb4)
    YYbd4(i)=0-YYb4(i);
    shiftBA4(i)=BA4(i+1199)+YYbd4(i);
    transBA4=transpose(shiftBA4);
end

xb5=[1200 1203 1312 1380 1414 1783 1817 1882 1990 2000 2100 2200];
yb5=[BB5(1200) BB5(1203) BB5(1312) BB5(1380) BB5(1414) BB5(1783) BB5(1817) BB5(1882) BB5(1990)
BB5(2000) BB5(2100) BB5(2200)];  %
p5=polyfit(xb5,yb5,4);
Xb5=1200:2200;
Y5=polyval(p5,Xb5);                                          % Auto-correlation 5
for i=1:length(Y5)
    Yd5(i)=0-Y5(i);
    shiftBB5(i)=BB5(i+1199)+Yd5(i);
    transBB5=transpose(shiftBB5);
end

xxb5=[1200 1207 1313 1879 1990 2000 2100 2200];
yyb5=[BA5(1200) BA5(1207) BA5(1313) BA5(1879) BA5(1990) BA5(2000) BA5(2100) BA5(2200)];
pp5=polyfit(xxb5,yyb5,3);
XXb5=1200:2200;
YYb5=polyval(pp5,XXb5);                                  % Cross-correlation 5
for i=1:length(YYb5)
    YYbd5(i)=0-YYb5(i);
    shiftBA5(i)=BA5(i+1199)+YYbd5(i);
    transBA5=transpose(shiftBA5);
end

xb6=[1200 1203 1312 1380 1414 1783 1817 1882 1990 2000 2100 2200];
yb6=[BB6(1200) BB6(1203) BB6(1312) BB6(1380) BB6(1414) BB6(1783) BB6(1817) BB6(1882) BB6(1990)
BB6(2000) BB6(2100) BB6(2200)];
p6=polyfit(xb6,yb6,4);
Xb6=1200:2200;
```

```
Y6=polyval(p6,Xb6);                                                    % Auto-correlation 6
for i=1:length(Y6)
      Yd6(i)=0-Y6(i);
      shiftBB6(i)=BB6(i+1199)+Yd6(i);
      transBB6=transpose(shiftBB6);
end

xxb6=[1200 1207 1313 1879 1990 2000 2100 2200];
yyb6=[BA6(1200) BA6(1207) BA6(1313) BA6(1879) BA6(1990) BA6(2000) BA6(2100) BA6(2200)];
pp6=polyfit(xxb6,yyb6,3);
XXb6=1200:2200;
YYb6=polyval(pp6,XXb6);                                                % Cross-correlation 6
for i=1:length(YYb6)
      YYbd6(i)=0-YYb6(i);
      shiftBA6(i)=BA6(i+1199)+YYbd6(i);
      transBA6=transpose(shiftBA6);
end

%-------------------------------------------------------------------------%
%                          NORMALIZATION                                  %
%-------------------------------------------------------------------------%
maxAA=max(transAA1);
maxBB=max(transBB1);
normtransAA1=transAA1/maxAA;
normtransBB1=transBB1/maxBB;
normtransBA1forA=transBA1/maxAA;
normtransBA1forB=transBA1/maxBB;
```

8 CURRICULUM VITA

Joel Quintana was born on October 5th, 1981 in El Paso, Texas. He is son to Rosalia Quintana and Rafael Romero, younger brother to Juan Rene Quintana. Joel is the first in his family to receive an advanced degree from a nationally accredited university. Joel attended and graduated from El Paso High School in 2000. Upon graduation Joel attend the University of Texas at El Paso receiving a Bachelors of Science in Electrical Engineering degree in December of 2006. While an undergraduate, Joel participated in many electrical engineering internships with Lockheed Martin. During his internship term Joel designed a Point to point Fiber Optic System still used by the test team at Lockheed Martin Missile and Fire Control. Joel continued his education at UTEP receiving a Masters of Science in Electrical Engineering in May of 2009. Joel has accepted a job offer with Raytheon Integrated Defense Systems located at White Sands Missile Range New Mexico.

Permanent Address: 7101 Luz De Espejo Dr.
El Paso, TX 79912